Universidade de Aveiro Departamento de
2020 Eletrónica, Telecomunicações e Informática

Joaquim Melim

Implementação e Avaliação em System Generator de um Sistema Cooperativo para os Futuros Sistemas 5G

Implementation and Evaluation on System Generator of a Cooperative System for 5G Future Systems

This work is supported by the European Regional Development Fund (FEDER), through the Competitiveness and Internationalization Operational Program (COMPETE 2020) of the Portugal 2020 framework, Regional OP Centro (CENTRO 2020), Regional OP Lisboa (LISBOA 14-20) and by FCT/MEC through national funds, under Project MASSIVE5G (AAC no 02/SAICT/2017)

Joaquim Melim

Implementação e Avaliação no System Generator de um Sistema Cooperativo para os Futuros Sistemas 5G

Implementation and Evaluation on System Generator of a Cooperative System for 5G Future Systems

Dissertação apresentada à Universidade de Aveiro para cumprimento dos requisitos necessários à obtenção do grau de Mestre em Engenharia Electrónica e Telecomunicações, realizada sob a orientação científica do Doutor Professor Manuel Violas, Professor Auxiliar da Universidade de Aveiro do Departamento de Eletrónica, Telecomunicações e Informática da Universidade de Aveiro, e do Doutor Professor Adão Silva, Professor Auxiliar da Universidade de Aveiro do Departamento de Eletrónica, Telecomunicações e Informática da Universidade de Aveiro

o júri / the jury

presidente / president	Professor Doutor Armando Carlos Domingues da Rocha Professor Auxiliar, Universidade de Aveiro
vogais / examiners committee	Professor Doutor Paulo Jorge Coelho Marques Professor Adjunto, Instituto Politécnico de Castelo Branco
	Professor Doutor Manuel Alberto Reis de Oliveira Violas Professor Auxiliar, Universidade de Aveiro

agradecimentos / acknowledgements

Em primeiro lugar gostaria de agradecer aos meus pais pelo apoio e paciência durante o meu percurso académico, e especialmente por me terem proporcionado esta enorme oportunidade de estudo.

Gostaria também de agradecer ao meu orientador Professor Manuel Violas e ao meu co-orientador Professor Adão Silva pelo apoio, ajuda, supervisão e revisão do meu documento com as suas opiniões de especialistas. Esta dissertação segura-se sobre vários anos de trabalho realizado por ambos nesta área. Sem os seus esforços os resultados obtidos durante este trabalho seriam virtualmente inalcançáveis.

Agradeço também aos amigos que estiveram ao me lado durante o meu percurso, pelo apoio moral, ajuda e conselhos. Sem eles estes anos teriam sido muito mais árduos e infelizes. Dos meus amigos, gostaria de agradecer em especial aos meus colegas Rafael Almeida e Samuel Simões, como também aos meus colegas do grupo de Wireless Communications, por me terem aconselhado e ajudado durante este último esforço. Estendo os meus agradecimentos à Karolina Bezler, à Meghan Foster e à Ana Barreiros pelo apoio moral nos últimos meses.

Por fim, agradeço à Universidade de Aveiro, ao Departamento de Eletrónica, Telecomunicações e Informática e ao Instituto de Telecomunicações por fornecerem as condições necessárias de trabalho e aprendizagem.

Palavras-chave 5G, redes heterogéneas, HetNets, Alinhamento de Interferência, Sistema Cooperativos, System Generator

Resumo Com a chegada do 5G, espera-se a proliferação de serviços nas mais diversas áreas tal como assistência médica, automação industrial, transmissão em 4k, que não eram possíveis nas redes das gerações anteriores. Além deste fenómeno, o número total de dispositivos capazes de conexões wireless aumentará de tal maneira que a escassa largura de banda disponível não será suficiente para abranger os objetivos pretendidos. O Relatório Anual de 2018 sobre a Internet da Cisco prevê que até 2023 haverá quase 30 bilhões de dispositivos capazes de comunicação sem fio. Devido ao aumento exponencial de serviços e dispositivos, os desafios sobre a capacidade de dados da rede e o udo eficiente dos recursos de rádio serão maiores que nunca. Por estes motivos, a necessidade de soluções para estas lacunas é enorme.

Tanto a capacidade da rede e o uso eficiente do espectro de frequências estão relacionados ao tamanho da célula e à proximidade dos usuários com o ponto de acesso da célula. Ao encurtar a distância entre o transmissor e o recetor ocorre um melhoramento destes dois aspetos da rede. Este é o principal conceito na implementação de redes heterogéneas, HetNets, que são compostas por diversas células pequenas que coexistem na área de uma macro célula convencional, diminuído a distância entre os utilizadores da célula e os pontos de acesso, garantindo uma melhor cobertura e taxa de dados mais elevadas. No entanto, o potencial das HatNets não vem sem nenhum custo, pois estas redes sofrem consideravelmente de interferência entre as células.

Embora nos últimos anos foram propostos alguns algoritmos que permitem a coexistência das células, a maioria destes foi só testado em simulações de software e não em plataformas em tempo real. Por esse motivo, esta dissertação de mestrado visa dar o primeiro passo na implementação e a avaliação de uma técnica de mitigação de interferência em hardware. Mais especificamente no cenário de *downlink* entre uma estação base de uma macro célula, um utilizador primário da macro célula e um utilizador secundário de uma célula pequena, com o principal objetivo de cancelar a interferência que a estação base possa fazer ao utilizador secundário. O estudo foi realizado utilizando a ferramenta System Generator DSP, que é uma ferramenta que gera código para hardware a partir de esquemáticos criados na mesma. Esta ferramenta também oferece uma vasta gama de blocos que ajudam a criação, e fundamentalmente, a simulação e o estudo do sistema a implementar antes de ser traduzido para hardware. Os resultados obtidos neste trabalho são uma fiel representação do comportamento do sistema implementado. O quais podem ser utilizados para uma futura aplicação para FPGA.

Keywords 5G, heterogeneous networks, HetNets, Interference Aligment, Cooperative Systems, System Generator

Abstract

With the arrival of 5G it is expected the proliferation of services in the different fields such as healthcare, utility applications, industrial automation, 4K streaming, that the former networks can not provide. Additionally, the total number of wireless communication devices will escalate in such a manner that the already scarce available frequency bandwidth won't be enough to pack the intended objectives. Cisco's Annual Internet Report from 2018 predicts that by 2023 there will be nearly 30 billion devices capable of wireless communication. Due to the exponential expiation of both services and devices, the challenges upon both network data capacity and efficient radio resourse use will be greater than ever, thus the urgency for solutions is grand.

Both the capacity for wireless communications and spectral efficiency are related to cell size and its users proximity to the access point. Thus, shortening the distance between the transmitter and the receiver improves both aspects of the network. This concept is what motivates the implementation of heterogeneous networks, HetNets, that are composed of many different small-cells, SCs, overlaid across the same coexisting area of a conventional macro-cell, shortening the distance between the cell users and its access point transceivers, granting a better coverage and higher data rates. However, the HetNets potential does not come without any challenges, as these networks suffer considerably from communication interference between cells.

Although some interference management algorithms that allow coexistence between cells have been proposed in recent years, most of them were evaluated by software simulations and not implemented in real-time platforms. Therefore, this master thesis aims to give the first step on the implementation and evaluation of an interference mitigation technique in hardware. Specifically, it is assumed a downlink scenario composed by a macro-cell base station, a macro-cell primary user and a small cell user, with the aim of implementing an algorithm that eliminates the downlink interference that the base station may cause to the secondary users. The study was carried out using the System Generator DSP tool, which is a tool that generates code for hardware from schematics created in it. This tool also offers a wide range of blocks that help the creation, and fundamentally, the simulation and study of the system to be implemented, before being translated into hardware. The results obtained in this work are a faithful representation of the behavior of the implemented system, which can be used for a future application for FPGA.

List of contents

List of figures

List of tables

List of acronyms

1G	Fisrt Generation.
2G	Second Generation.
3G	Third Generation.
3GPP	Generation Partnership Project
4G	Forth Generation.
5G	Fifth Generation.
ABS	Almost Blank Subframes
ADSL	Asymmetric Digital Subscriber Lines
AMPS	Advanced Mobile Phone System
APs	Access Points
AWGN	Additive white Gaussian noise
BER	Bit Error Ratio
BPSK	Binary Phase Shift Keying
BRAM	Block Rams
BS	Base Station
CDMA	Code Division Multiple Access
CoMP	Coordinated Multi-Point
CP	Cycle Prefix
CRS	Common Reference Signals
CSI	Channel Side Information
CU	Control Unit
D2D	Device to Device
DoFs	Degrees of Freedom
DSL	Digital Subscriber Line
DSP	Digital Signal Processors
EDGE	Enhanced Data rates in GSM Environment

FDD	Fime-Division Duplexing
FDM	Frequency-Division Multiplexing
FDMA	Frequency Division Multiple Access
FF	Flip Flops
FFR	Fractional Frequency Reuse
FFT	Fast Fourier Transform
FIFO	First in First out
FR	Frequency Reuse
GPRS	General Packet Radio
GSM	Global System for Mobile Communication
HDL	Hardware Description Language
HetNets	Heterogeneous Networks
HSPA	High-Speed Packet Access
IA	Interference Alignment
ICI	Intercell Interference
IFFT	Inverse Fast Fourier Transform
IO	Input-Output blocks
IoT	Internet of Things
IoV	Internet of Vehicles
IP	Internet Protocol
IP	Intellectual Property
ISI	Inter Symbol Interference
LFSR	Linear Feedback Shift Register
LOS	Line of Sight
LTE	Long Term Evolution
LTE-A	LTE-Advanced
LUT	Look-up-tables
LUTRAM	Look-Up Table as Distributed Ram
M2M	Machine to Machine
MIMO	Multiple Input Multiple Output
MISO	Multiple-input Single-output
MMS	Multimedia Message Service
mmWave	Millimeter wave
MUT	Macro-cell User Terminal
NTT	Nippon Telephone and Telegraph

OFCDM	Orthogonal Frequency and Code Division Multiplexing
OFDM	Orthogonal Frequency Division Multiplexing
OFDMA	Orthogonal Frequency Division Multiple Access
PAPR	Peak-to-Average Power Ratio
Pe	Probability of Error
QAM	Quadrature Amplitude Modulation
Qof	Quality of Service
QPSK	Quadrature phase-shift keying
RF	Radio Frenquency
RN	Relay Nodes
SC	Small-cell
SC-FDMA	Single Carrier FDMA
SIMO	Single-input Multiple-output
SMS	Short Message Services
SNR	Signal-to-Noise Ratio
STBC	Space-Time Block Codes
TDD	Time-Division Duplexing
TDMA	Time Division Multiple Access
UTs	User Terminals
WCDMA	Code Division Multiple Access

Chapter 1

Introduction

In this chapter will briefly introduce the history of radio communications and specify what each generation brought or will bring to the wireless communication world. Subsequently, the motivations and objectives of this work will be presented, to then close this chapter with the document outline.

1.1 History of mobile telecommunications

Inevitably, this master thesis will start with a brief history of wireless communications, as studying its history is a necessary step to take, in order to understand that the current state of our telecommunications is neither accidental nor arbitrary, but a proof that there is always more possibilities of improvement than we can imagine. In the beginning, one of the first methods of communicating wirelessly was via smoke signals, that would allow humans to transmit news or warning messages between each other, without a physical connection. However, the wireless communications that we know today started with the understanding of the magnetic and electric properties of our planet. From the discovery of electromagnetic induction by Faraday in 1831, to Maxwell that formulated the first equations for electromagnetic waves in 1864, were some of the first discoveries that helped to recognize the existence of electromagnetic waves. Step by step through the 19th century, these men studies, and many others, led to Marconi's wireless telegraph and the first voice communication cross Atlantic on the turn of the 20th century.

The first commercial automated cellular network was deployed in Japan by Nippon Telephone and Telegraph (NTT) in 1979, establishing what would be the first generation (G) of telecommunications, 1G. After this point, the wireless communications begun to be numbered by generations that would change with the decade. Each generation brings some change on its standards, capacities and techniques that improves its overall performance relatively to the previous one [1].

1G

The first generation begun with the implementation of the first wireless mobile communication systems and the launch of the first cell phone by Motorola, the model DynaTAC 8000X pioneered by Martin Cooper, in the early 1980s. The first country to provide a nationwide network was Japan by NTT, that would then be followed by several other nations such as the Scandinavian countries, USA, Mexico, UK and Canada. 1G offered only voice service, based on Advanced Mobile Phone System (AMPS), that was an analog technology. The AMPS was frequency modulated and used Frequency Division Multiple Access (FDMA), with a channel capacity of 30KHz, allocated on the frequency band around 824-894MHZ, and it could achieve data rates of 2.4kbps [1]. As this technology was entirely analog, the Quality of Service (Qof) was not optimal due to its technological limitations [2][3].

2G

The second generation was a big turning point in wireless technologies, especially due to the transition from the 1G analog systems to the new digital technology, that was introduced in the late 1980s. 2G brought new services such Short Message Services (SMS), Multimedia Message Service (MMS) and also Internet access. This generation used a bandwidth of 30-200KHz and used digital signals to voice transmission, that could reach speeds up to 64kbps [1][3]. 2G also standardized digital modulations schemes, such as Time Division Multiple Access (TDMA) and Code Division Multiple Access (CDMA), that would allow the access of more users simultaneously. With the introduction of TDMA, the system could now divide multiple data streams into different time slots, while CDMA would grant multiplexing gain, since each user could use a unique code to communicate over a multiplexed channel. Although different standardizations were created from TDMA. GSM used both FDMA and TDMA modulation and was the first system to provide roaming which allowed its users to use their mobile phone in different countries, without sacrificing to much the Qof [2]. The 2G is considered to be one of the most successful generations, as it created an exponential increment in wireless communications users in the 1990s. The exponential growth in mobile telecommunication systems and users led to development of the 2.5G system, that lied between 2G and 3G. This system achieved data rates of 144kps [1] and introduced the General Packet Radio (GPRS) and Enhanced Data rates in GSM Environment (EDGE), that would provide more services and enhance the overall performance of 2G, being a significant step towards 3G [4].

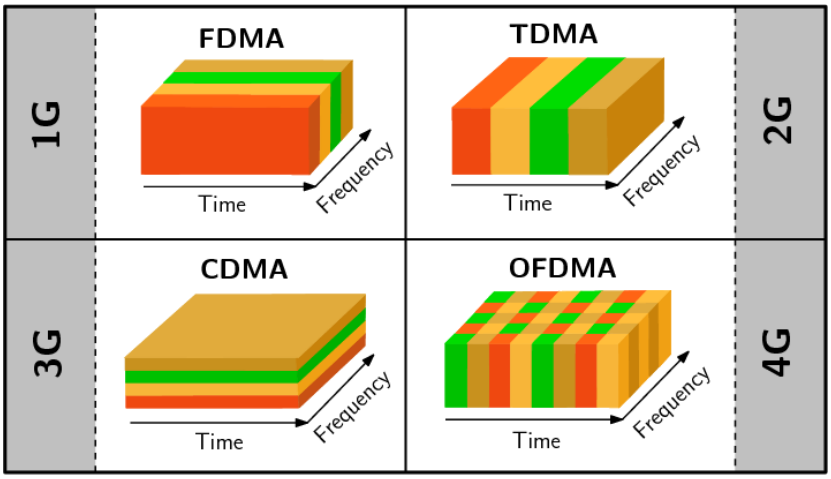

Figure 1.1: Signal Modulations for the Generations [5].

3G

The third generation begun in the 2000s, with the main goal of increasing data rates up to 2Mbps, coverage, and offer more overall services. 3G offered advanced multimedia services that were much greater than the ones granted by the former 1G and 2G. This generation offered internet access like none other generation before, as most of its packets included data services that opened the door for many capabilities such as, Web browsing, e-mail, video streaming and navigation maps, that were not easily available before [1]. Besides, with the launch of smartphones by the end of the 20000s, these services became mundane [3]. These functions were widely available due to 3G's data rate speed of 144-384kps in wide coverage areas and 2Mbps in local areas, along with a bandwidth of 5MHz [2]. Unlike 2G, 3G developed more towards CDMA techniques and standardization than TDMA, creating Wide band Code Division Multiple Access (WCDMA). WCDMA can achieve greater data rates, up to 2Mbps, and used more bandwidth, 5MHz, compared to CDMA's 144kbps speed and 1.2MHz of channel capacity. The standardization of WCDMA was done by an organization called 3rd Generation Partnership Project (3GPP). After this decade 3GPP would become one of the most influential standard development body of cellular communications in the world, being also present in the implementation of the future generations, 4G and 5G. Towards the late 2000s WCDMA evolved to High-Speed Packet Access (HSPA) that could achieve transmission speeds up to 8-10Mbps [3]. 3G also brought the concept of Multiple Input Multiple Output (MIMO) systems that could reach data rates of 42Mbps [6], nevertheless, MIMO systems would be widely implemented in the following generation, 4G.

4G

Unlike the previous generations, 4G or Long Term Evolution (LTE), development was not as linear and innovative as its counterparts. The fourth generation started to be implemented in 2010, and its main goal was to enhance the former services brought by the 3G, making them faster, more robust, and accessible to more users, by bringing the concept of ubiquitous connectivity, that would be available at anytime, anywhere and from any kind of device while offering high data rates. To provide higher capacity, quality and speed on its multimedia and internet applications, while keeping a low cost on its data services, 4G network was adapted to Internet Protocol (IP). The transition to IP was done in order to establish a common platform for all technologies [1]. Besides, this generation exploited both CDMA and Orthogonal Frequency Division Multiplexing (OFDM) for its signal modulation. OFDM was introduced by 4G and had higher spectral efficiency and good anti-multipath interference, it improved the utilization of bandwidth compared to CDMA, which not only increased the capacity of systems, but also meet the requirements set for the multimedia communications[7]. 4G used particularly two extensions of OFDM, Orthogonal Frequency Division Multiple Access (OFDMA) and Single Carrier FDMA (SC-FDMA) that were implemented for downlink and uplink connections, respectively. LTE also adopted a general use of multiple antenna systems, in particular MIMO systems that were used to increase its transmission quality and robustness against interference. Both OFDM and MIMO technologies will further be explained in chapter 2. LTE uses the spectrum band around 2000 Mhz to 8000 Mhz and has channel bandwidth of 5Mhz to 20 MHz, it can also achieve a maximum downlink speed of around 100 Mbps and uplink speed of around 50 Mbps [6]. However, these specifications did not compliant with the International Telecommunication Union's requirements for IMT-Advanced of 600Mbps for downlink and 270Mbps for uplink with along with a bandwidth of 40MHz [8][9]. Thus, an enhanced LTE was release called LTE-Advanced (LTE-A), which by focusing on carrier aggregation, relaying and enhancements to multiple antenna transmission on the uplink and downlink achieved a maximum bandwidth of 100MHz and a maximum data rate of 1Gbps for the downlink and 500Mbps that surpass the expectations for IMT-Advanced[8].

5G

The current year, 2020, is the starting point of the fifth generation 5G, which has already been deployed in some cities in countries all over the world[10] and promises to be more disruptive and innovative than the former two generations[11][12]. Unlike the third and fourth generations, that focused on improving the speed and efficiency of wireless networks, 5G promises to spread and establish wireless communications on distinct application fields that nowadays network still struggle to implement[11]. These fields include wireless healthcare services, utility applications, industrial automation, virtual and augmented reality services, 4K streaming, machine-to-machine communication, etc[13]. Above all these new services,

it expected that the new technologies will investigate the challenges within each field to provide a performance with low latency, high speed, enhanced reliability, peak throughput per connection, system spectral efficiency, connection, and capacity density, and low power consumption [14][13]. According to this to [15] and this report released by Nokia [16], 5G goals and requirements to provide the proposed services should be as follow:

- 10 Gbits/s peak data rate.
- 1 millisecond latency.
- Low cost for M2M communication.
- 1000 times more data traffic.
- 100 Mbit/s speed at minimum coverage.
- 10-year M2M battery life.

With the expansion of services and the objectives set for this generation, there are two significant physical challenges that need to be addressed headmost, and they are the massive increment of data traffic and the scarcity of available channels in the frequency spectrum. With the new Ultra-High-Definition, 4K, video streaming capacities, an HD television with internet connection streaming three hours of content per day from the Internet, would generate as much Internet traffic as an entire household would in 2018[17]. Adding to this factor, Cisco's Annual Internet Report from 2018 predicts an increase of up to 5.3 billion internet users by 2023 [17] which will only exponentially increase the data traffic. When it comes to the frequency spectrum its channel scarcity will be linked with the growth of wireless transceivers needed to provide services such as home automation, factory automation, vehicle diagnostics, navigation, and many others[13] [15]. To tackle the mention challenges, 5G brings new technologies that will change the core network of the existing 4G system. Some of those technologies are as follow:

1. Millimeter wave (mmWave): One of the answers for the lack of channels is to use higher frequencies of the frequency spectrum the Millimeter waves. This side of the spectrum is still mostly available and it ranges from 3 to 300 GHz[11][18]. As most of that part of the spectrum is not being used, there is the possibility of allocating larger bandwidth to its applications allowing for higher data rates. Although promising, mmWaves are more affected by shadowing and pathloss compared to the microwaves[19][20]. However, this technology can be combined with both multiple antenna arrays and multiple cell architecture networks in order to overcome its pathloss challenges.

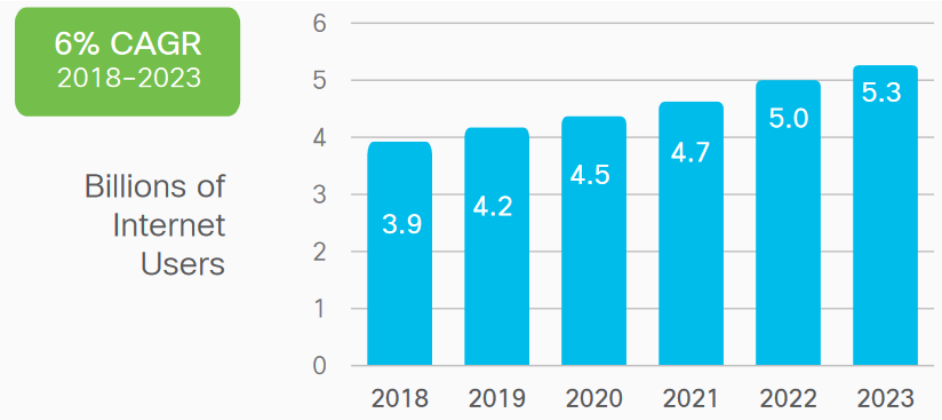

Figure 1.2: Cisco Annual Internet Report forecast of the number of Internet users , until 2023.[17].

2. Massive MIMO: Massive MIMO consists on using a large number of antennas in a single transmitter, in order to multiplex messages for several devices on each time-frequency resource, increasing the data throughput, while also exploiting all the other advantages of MIMO[21]. On the 5G network, this concept is going to be applied to the network's base stations. As the frequencies to be implemented on this generation are around the GHz, this means that the antennas can be especially small allowing the aggregation of multiple antenna arrays up to more than 100 elements. Massive Mimo also enables the use of beamforming, which allows the transmissions to be directed with precision to the user in order to mitigate the pathloss and shadowing effects of the mmWaves[11][20].

3. Small-cell (SC): The deployment of small-cells closer to the users, within the coverage area of a base station macro-cell, can improve both the network data traffic capacity, increase its spectral efficiency and also offload the data traffic from the main base stations of the macro-cells enabling a greater QoF[22][23]. SCs are usually related to the concept of Heterogeneous Networks (HetNets) [22][23][20]. This concept promotes the creation of a multiple-cell network, with the objective of establishing an environment of coordination between the different terminals, thus enabling a higher network capacity and a higher efficiency of the radio resources utilization[23][24]. Additionally, the addition of more access points throughout the macro-cell can also mitigate the pathloss and shadowing effects on the mmWaves, as the transceivers are deployed with the objective of covering any existing blind spots on the cell area. However, the cell densification of the HetNets may cause extreme interference between cells that calls for more complex interference mitigation techniques, as well as higher demand for backhaul links and shared information between the cells.

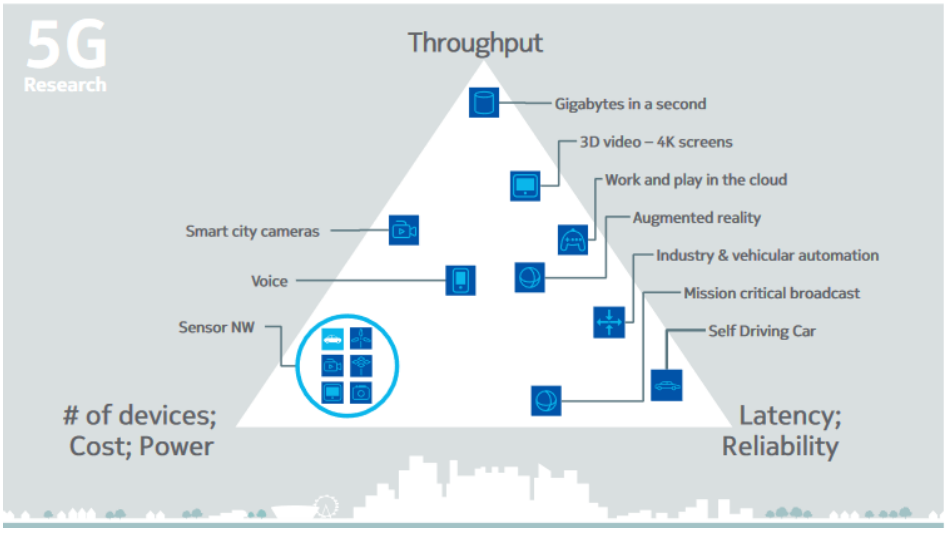

Figure 1.3: Pyramid of emerging services brought by 5G[16].

Although the previously mention technologies can be considered the most disruptive and critical, when it comes to changing the 4G network core and its data capacity, there are also other technologies that may contribute to the efficiency and services of the future 5G networks. Concepts such as Device to Device (D2D), Internet of Things (IoT), Internet of Vehicles (IoV) and Machine to Machine (M2M) will grant the majority of the emerging services in the different fields as previously mention[11].

1.1.1 Motivation

With the proliferation of services in the different fields (such as healthcare, utility applications, industrial automation, 4K streaming) that are to be delivered by the 5G network, the total number of wireless communication devices will escalate in such manner that the already scarce available frequency bandwidth won't be enough to pack all the new incoming systems[11][20]. Cisco's Annual Internet Report from 2018[17] predicts that by 2023 there will be nearly 30 billion devices capable of wireless communication, as shown in figure 1.4, which would be roughly 10 billion more devices compared to 2018 figures. Due to the exponential growth of both services and devices, the challenges upon both network data capacity and efficient radio recourse will be greater than ever, as the 4G network, cant provide[12] the needed capacity nor the conventionally use of the frequency band spectrum is efficient enough. Both the capacity for wireless communications and spectral efficiency are related to cell size and its users proximity to the access point [25]. Thus, shortening the distance between the transmitter and the receiver improves both aspects of the network. This concept is what motivates the implementation of HetNets, that are composed by many different small-cells, SCs,(with coverage within 100 meters) overlaid across the same coexisting area of a conventional macro-cell (with coverage higher than 500m), thus shortening the

distance between the cell users and its access point transceivers, granting a better coverage and higher data rates [22]. As the SCs are to be deployed within the macro-cell area, they can be used to offload the data traffic from the macro-cell base station on its hot spots while communicating over the same frequency band as the base station. The HetNets potential does not come without any cost or challenges, as these networks suffer considerably from communication interference between cells. Therefore, there is still room for improvement and research to be done on this field. Recently, some interference ligament algorithms that allow coexistence between the small-cells (secondary users) and the macro-cell (primary users) have been proposed [26] [27]. However, most of the proposed schemes were evaluated by software simulations and not implemented in real-time platforms. Therefore, this master thesis aims to give the first step on the implementation and evaluation of an interference mitigation technique in hardware. Specifically, we consider a macro-base cell with a base station and a primarily user and two small-cells with one secondary user each, and the primary objective is to implement and algorithm that eliminates the downlink interference that the base station may cause to the secondary users. Both the implementation and evaluation of this technique will be done by creating Intellectual Property (IP) using the hardware modeling toll System Generator. Thus, conceiving the foundation for future hardware implementation.

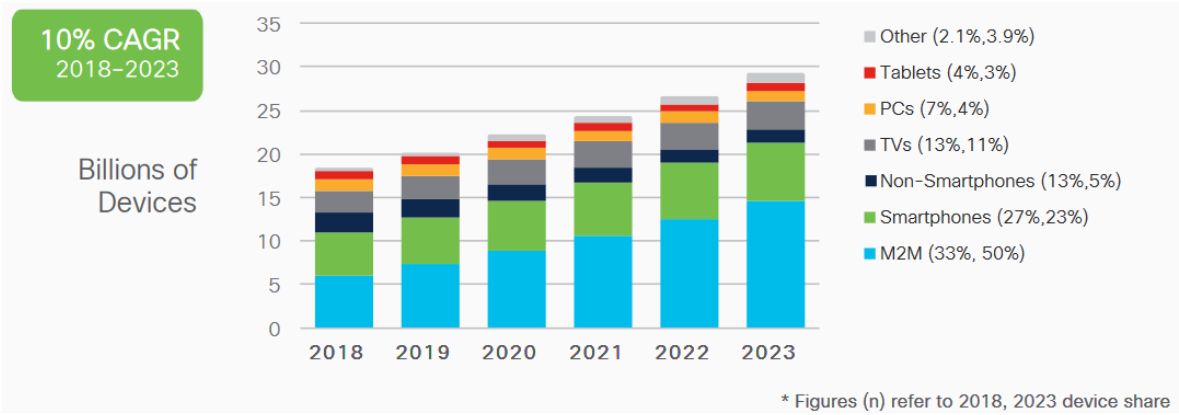

Figure 1.4: Cisco Annual Internet Report forecast of the number of devices, until 2023.[17].

1.1.2 Outline

The rest of this document is structured as follows:

Chapter 2: This chapter overviews the most important concepts relative to the scope of this master thesis. The chapter begins with a brief explanation of both the signal modulation OFDM, that was implemented in our model, and also the use and benefits of Multiple Antennas Systems. Subsequently, an overview and definition of the conventional cellular network structure as well as the SCs and the HetNets, where we will also characterize their challenges and requirements, with emphasis on the HetNets interference management. This chapter ends with the analysis of one of the different interference management methods proposed for the HetNets, the Interference Alignment .

Chapter 3: In this chapter, we present interference alignment algorithms recently proposed. First, it is presented the general system model along with three different methods of Interference Alignment (Static method, Coordinated method, Two-bit method) with different requirements in terms of channel state information feedback. Then, we describe the simplified model and algorithms implemented in hardware. Finally, this chapter ends with a detailed explanation of the mathematical manipulation done for hardware implementation.

Chapter 4: This chapter begins by introducing the main tool used to accomplish this work, System Generator for DSP, which is a modeling tool for hardware designing. Subsequently, there is the description of the transmitting and receiving schemes used to transmit the data signals. These two schemes establish a reliable OFDM modulated transmission between the transceivers and were the basis of the entire design. Then, it will be explained, with more detail, the designs conceived specially for this thesis, that were created to implement the IA method proposed in this thesis. This chapter ends with the description of the tests done to each of the created designs a long with their respective results.

Chapter 5: The final chapter concludes the master thesis with the summary of the main results and the proposition for some future lines of work.

Chapter 2

Preliminar Insight

This chapter presents a brief overview of the main theoretical concepts of the topics relative to this thesis. First, we will do a brief introduction on OFDM modulation along with multiple antennas systems. Then, the conventional cellular architecture is presented followed by the definition and major advantages of HetNets. As the concept of HetNets has challenges mainly related to the interference management. Since the HetNet architecture consists of two tiers (macro-cell and small-cells) where these two systems have to coexists over the same spectrum resulting in considerable interference, hence degrading the performance of both the systems. Therefore, in this chapter it is also presented some of the proposed methods to manage the interference on HetNets, with more emphasis in the Interference Alignment technique.

2.1 Signal modulation OFDM

Orthogonal Frequency Division Multiplexing is a method of signal modulation that divides a data stream by multiple carriers. Each symbol of the data stream is transmitted in parallel, with its assign sub-carrier through its own channel, allowing the transmission of a high bit rate sequence through different low rate streams. This modulation is a variation of Frequency-Division Multiplexing (FDM), with the difference of utilizing sub-carriers that are closer and orthogonal to each other in the frequency domain, allowing for a more efficient use of the frequency spectrum while minimizing both interference and crosstalk[28]. OFDM is versatile as it can be applied along with different digital modulation techniques as BPSK, QPSK, QAM and so on[29]. The performance of OFDM relies on the orthogonality of each sub-carrier and the spacing between them. Considering that the transmitted signal is allocated to a bandwidth of B, the data symbols are then distributed by a Nc number of sync sub-carriers. To guarantee the orthogonality between subcarriers, each sync is separated by a ratio Δ_{f_p} determined[30]:

$$\Delta f_p = \frac{B}{N_c} \tag{2.1}$$

The relationship between the symbol duration, T_s, and the sub-carriers spacing, can be expressed as:

$$T_s = \frac{1}{\Delta f_p} \tag{2.2}$$

Orthogonality is achieved when the maximum peak of each sub-carrier corresponds to a zero of all the overlapping syncs in the frequency domain, just as it's illustrated in figure 2.1. The modulation of these signals into an OFDM symbol, is usually done by utilizing Inverse Fast Fourier Transform (IFFT) algorithms, while the demodulation is done with Fast Fourier Transform (FFT) algorithmsused[30].

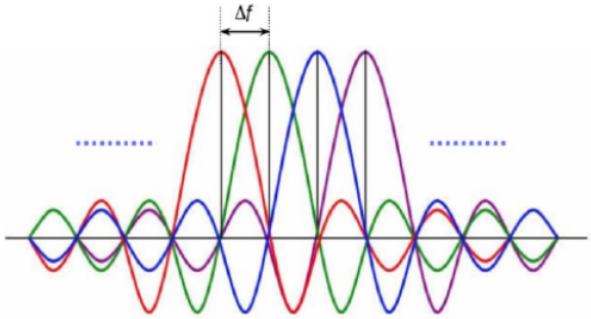

Figure 2.1: The orthogonality concept in OFDM[31].

To eliminate, almost completely, the existence of Inter Symbol Interference (ISI), and Inter Carrier Interference, ICI, that may be caused by delay dispersion from the propagation channels, it's added a Cycle Prefix (CP) to every OFDM symbol. This added prefix is usually part of the tail of the symbol. To achieve an ISI free transmission, the duration of the CP as to be equal to the time of the maximum path delay, $\tau_{\max}$, from the transmission channels. Thus, the real duration of a symbol is[30]:

$$T_{OFDM} \approx \frac{Nc}{B} + \tau_{\max} \tag{2.3}$$

OFDM is very popular and it has been used in several technologies over the decades. It was exploited in the 90's for FM radio channels and Asymmetric Digital Subscriber Lines (ADSL). In recent years it was used in wireless communication standards, such as Wi-Fi (IEEE 802.11a), WiMax (IEEE 802.16). Its principle was used to create both OFDMA and SC-FDMA that were implemented on 4G systems for downlink and uplink connections respectively [28][30]. The LTE standard specifications for OFDM are as follow:

Table 2.1: LTE standard OFDM specifications.

FFT size	1024
Number of sub-carriers (N_s)	768
Sample frequency	15.36MHz
OFDM symbol duration (T_{OFDM})	71.86μ
Cycle Prefix duration (CP)	66.6μ
Useful symbol duration	5.21μ
Sub-carrier separation (Δ_{f_p})	5.21μ

2.1.1 Transmission

The transmission and modulation of an OFDM signal, begins with the digital modulation of the transmitting data, into one of the single carrier techniques (QPSK, BPSK, QAM-16, etc...)[30]. The modulated data stream is then split into parallel sub-streams using a serial-to-parallel conversion block. The multi-carrier configurations are done after the split by an IFFT block, that converts the streams to the time domain. Following the conversion, the signal is again processed into a single stream by a parallel-to serial block. The CP, which usually is a copy of the end of the OFDM symbol, is then added to the beginning to the signal to eliminate both the ISI and the ICI. Finally, the digital signal is converted into analog to be transmitted.

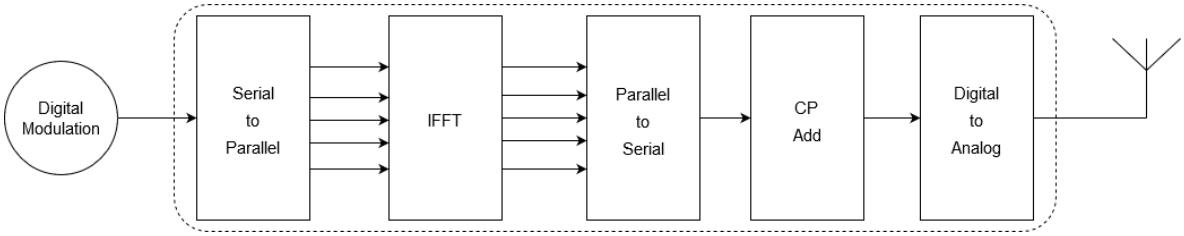

Figure 2.2: OFDM Modulation blocks.

2.1.2 Reception

The reception begins with the conversion of the analog signal to digital. Subsequently, the CP is removed so that the original OFDM symbol can be recovered. The stream is then split into parallel sub-streams, them number of sub-streams corresponds to the number of subcarriers used for the OFDM symbol, previously determined in the transmission. The FFT is calculated after the split, turning the signal into the frequency domain again. Before the final digital demodulation, the signal is transformed into a single data stream.

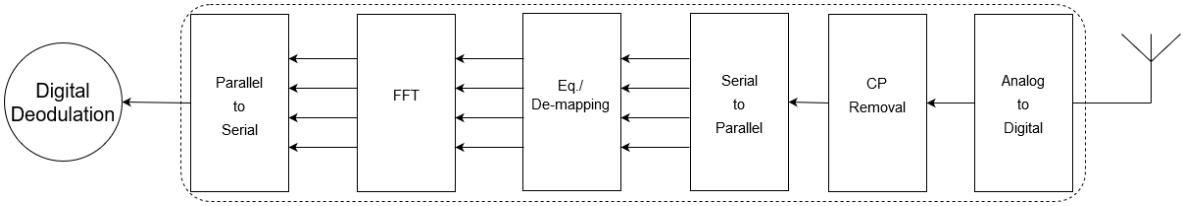

Figure 2.3: OFDM Demodulation blocks.

2.1.3 OFDMA

OFDMA is an extension of OFDM, that allows a multiuser communication system. OFDMA was used in LTE due to its good performance in selective fading channels, low complexity base-band receiver and compatibility with advanced receiver and antenna technologies, along with other qualities. OFDMA distributes sets of different subcarries per user[32]. The subcarries allocated to the user can either be in a continuous group or scattered along the OFDMA symbol bandwidth. As the users are divided in the frequency domain instead of the time domain, as in OFDM, OFDMA grants a simultaneous transmission to different users. As the transmission occur in the frequency domain, consisting in several parallel subcarriers, which in the time domain correspond to multiple sinusoidal waves with different frequencies that fill the symbol bandwidth with steps of 15 kHz. This causes the signal envelope to vary. As the symbols are sent simultaneously,the different sinusoids in the time domain may sum constructively leading to the creation of symbols with different peaks of amplitude, making the Peak-to-average-power-ration bad. To compensate this phenomenon, the amplifiers require additional back-off to keep working in a linear form and to prevent the problems to the output signal. This makes the amplifiers less power efficient. Due to its amplifier high power consumption, OFDMA was implemented on LTE multiple user downlink transmissions, as it was more suited to be used at base stations ratter than small mobile user devices[32]

2.1.4 SC-OFDMA

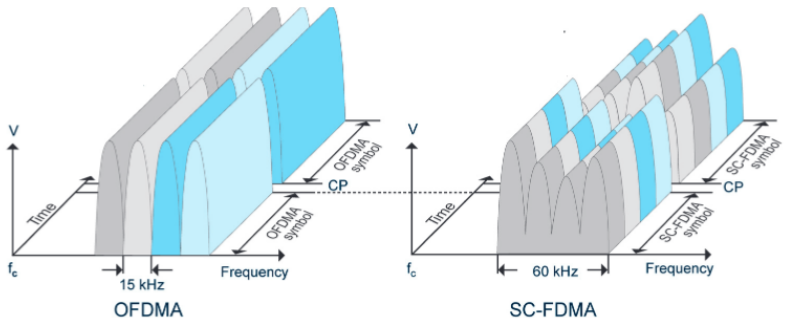

Figure 2.4: OFDMA and SC-FDMA signal modulation [33].

To improve the Peak-to-Average Power Ratio (PAPR) and increase both the efficiency of the power amplifiers and power consumption, SC-FDMA is used in LTE for the uplink transmissions. Unlike OFDMA, SC-FDMA does not allocate dedicated sub-carriers to each user, this modulation divides the different user symbols in the time domain, similar to the TDM techniques used in GSM[32]. The transmission occupies a continues part of the frequency spectrum allocated to the user, and a 1ms time slot of transmission, by the LTE standards, contrary to the OFDMA transmission where the user symbols are allocated in single carriers in the frequency domain while using longer periods of time, as represented in figure 2.4. Thus SC-OFDMA transmits in the time domain to a single user at a time while using multiple-subcarries in the frequency domain, contrary to what its name implies. Since the symbols are transmitted in the time domain, preforming a single modulation at a time, the signal envelopes properties and the waveform characteristics are determined by the modulation method applied[32]. This allows the SC-FDMA to reach a very low signal PAPR, achieving then a greater power use efficiency suited for the user mobile devices.

2.2 Multiple Antenna Systems

As wireless communications become mundane, the optimization of wireless systems is crucial to maximize the efficiency of both the RF spectrum and the communications Bit Error Ratio (BER), in order to save as much resources and expenses as possible. To tackle this problem, radio systems equipped with multiple antennas have been exploited over the last decades, due to their communication performance and bandwidth efficiency. There are different concepts of these systems and they can be listed as Single-input Multiple-output (SIMO), Multiple-input Single-output (MISO) and the previously mentioned MIMO, that are represented on figure 2.5. These systems achieve great transmission rates and spectral efficiency by exploiting the spatial gain provided by their multiple antennas used on their transceivers. The spacial gain can be roughly explain as multiple and simultaneous transmissions through different channels of the same signal, which happens when all the antennas are transmitting the same signal. Besides, the multiple antennas can also provide multiplexing gain, that is achieved when independent signals are transmitted and received simultaneously by each antenna of a multiple antenna system. In conjunction with the diversity that can be obtain by each single antenna, such as time diversity and frequency diversity, multiple antennas systems can also achieve transmission and reception diversity that can furthermore enhance the performance of these systems.

MIMO takes advantage of multiple antennas to transmit and receive parallel data streams, which allows it to benefit of both diversity and spatial multiplexing gain, depending on the methods used for transmission or reception [34][35].

Although this system needs different configurations to make the most of each property gain,

this does not mean that every MIMO is either purely maximized for multiplexing or diversity [35] [36]. Some systems try to obtain both gains by implementing coding schemes, that adjust the trade-off between the multiplexing and diversity gain, depending on its purpose[35]. For its versatility and degree of freedom, MIMO was integrated in most of the latest wireless communication technologies such as LTE [37], 3GPP2 Ultra Mobile Broadband, and IEEE 802.16 WiMAX [38]. Additionally, these systems are to be used even more intensely in the future, with the introduction of Massive MIMO by the 5G[39].

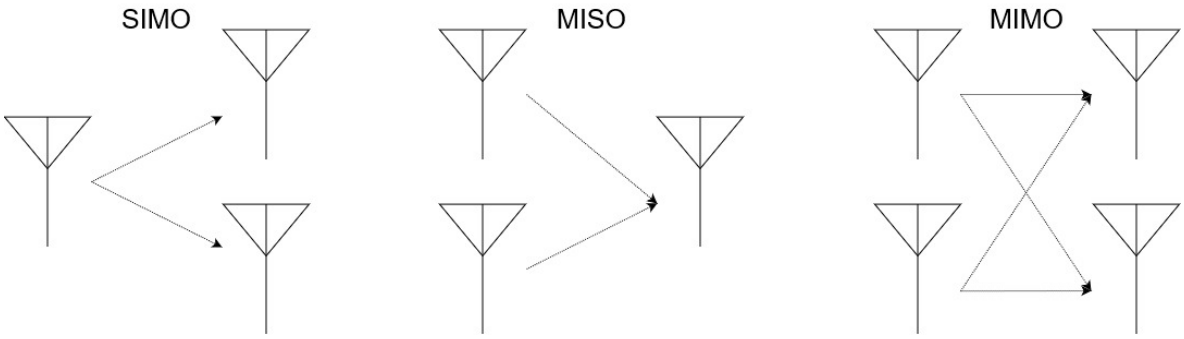

Figure 2.5: Spacial diversity systems.

2.2.1 Diversity

In communications systems, diversity refers to the transmission or reception of the same information by multiple paths that fade independently. The multiple paths can be separated in time, frequency and space, to subsequently be combined at the receiving end to create the radio transmission channel. As the paths are statistically independent, the likelihood of all of them suffering the same fading effect is very slim, thus the probability of acquiring a good quality channel is higher[34][35]. The transmission channels can be in a good state, wish means that they are reliable and their Signal-to-Noise Ratio (SNR) is high, or in a bad state, their SNR is to low to do a reliable connection. Considering channels with Rayleigh fading, the overall BER will be determined by the behavior of the bad state channels, thus we can assume, that the Probability of the a channel being bad is proportional to Probability of Error (Pe). Thus, the P_e is roughly given by

$$P_e \propto q, \tag{2.4}$$

where q, in a Rayleigh-fading environment, is proportional to $q = \frac{1}{SNR}$. Considering that the information is sent by L uncorrelated channels, if all the channels were in a bad state the P_e would be given by

$$P_e \propto q^L. \tag{2.5}$$

Thus, considering a Rayleigh-fading environment, where the probability of error, P_e, is proportional to the SNR:

$$P_e \propto \frac{1}{SNR}, \tag{2.6}$$

hence, with the increment of the number of path channels, L, through which the signal travels, reduces the P_e as it relates to L by:

$$P_e \propto \frac{1}{SNR^L} \tag{2.7}$$

It is noticeable, that with the addition of antennas it is possible to decay the average P_e without the need of increasing the transmission power, which is a great advantage. As mention before diversity gain can be obtained in time, frequency and space domain. The first two gains, time and frequency, can be designated as a single antenna diversity gain, as they are obtained according to the accommodation of the signal in time and in the frequency spectrum, while the space diversity depends entirely on the number of antennas used by the system.

Time Diversity

Time diversity is achieved by sending the same data stream, over separated periods of time. Each transmission must be separated by an interval greater than the coherence time, with the intent of letting the receiving signals suffer from different fading characteristics while traveling by the channels. This method, also referred as time interleaving, is usually applied in conjunction with coded data symbols. The transmitting symbols are rearranged and extended by an interleaving block before transmission. The symbols are extended for a duration greater than the slow deep fade period[40][41].

However, time interleaving reduces the data rate by the number of transmissions of the same signal. Adding to the last factor, this technique may suffer large delays when used on channels that slowly vary[42].

Frequency Diversity

Similar to the time diversity techniques, frequency diversity is achieved by transmitting the same narrow band signal through different carriers separated by the coherence band of the transmission channel. Its main drawbacks lay on the inefficient use of the Radio Frenquency (RF) spectrum, as this method usually requires more bandwidth, and also its ineffectiveness on channels where the coherence bandwidth is larger than the spreading bandwidth[42][36].

Spatial Diversity

Spatial diversity, as mention before, depends entirely on the number of antennas used by the system. Unlike the other diversity gains, its efficiency on acquiring independent paths

does not require more bandwidth nor the increment of the transmission power. This gain may be obtained not only with MIMO systems but also MISO or SIMO. If one of the ends of the wireless connection has more than one antenna it is possible to achieve this gain. However, the techniques used are different on both ends, dividing the spatial diversity as transmission and receiving diversities.

Receiving Diversity

At the receiver point, it is possible to take advantage of spatial gain, that is granted from the different fading coefficients from the paths acquired by the multiple receiving antennas, and antenna gain, granted by the independent noise terms from each received signal. These two gains must be combined in an efficient manner, and only MIMO and SIMO systems can benefit from them. If we consider a SIMO system, as depicted on figure 2.6, Mr represents the number of antenna branches of the receiver, where each branch receives an incoming signal y_{Mr}. Each y is composed by the transmitted symbol, s, the fading coefficient of the channel, h_{Mr}, and the antenna noise, n_{Mr}.

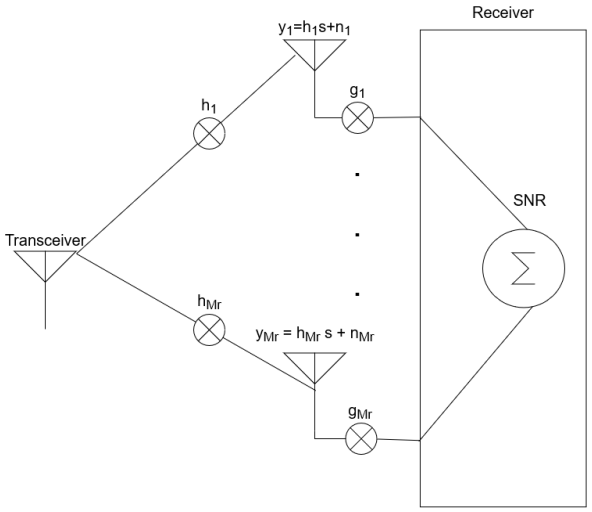

Figure 2.6: SIMO system, Receiving Diversity.

Transmitting Diversity

Transmission diversity is obtained when controlled redundancies are introduced at the transmission, therefore, the only systems able to exploit this gain are MIMO and MISO, as a minimum of two transmitting antennas is needed. Transmit diversity is mostly used in cellular systems, where most of the processing, power and space lays on the transmitter side, which is often a base station or an access point, in these systems. The methods to achieve this diversity diverge in two, either with Channel Side Information (CSI) or without CSI. The channel gains

may be obtained resorting to a backhaul link or a bi-directional communication scheme, that allow the share of information about the channel from the receiver to the transmitter. When the transmitter knows the channels, it is known as having channel side information, CSI. However, when this link it is not possible, the transmission is done by applying space-time coding without knowledge of the channel, such as the Alamouti's scheme.

With Channel Side Information

When the CSI exists at the transmitter side, the channel gains h_{Mr} can be used, for a more efficient power allocation to each transmitting antenna to create a beamforming transmission. The channel can be obtained by resorting to bi-directional systems, that separate the uplink and downlink operations, this separation is known as duplexing. Techniques such as Time-Division Duplexing (TDD), and Fime-Division Duplexing (FDD) grant the CSI as the channel information can be transmitted between uplink and downlink transmission[42].

The FDD uses different frequency bands to perform the uplink transmission and the downlink transmission, hence allowing both operations to occur simultaneously. A drawback of these systems occurs when the frequencies assigned to each direction are separated by more than the coherence bandwidth, resulting in a multipath channel diversity, hence not allowing CSI [42][43].

The TDD, uses the same frequency band and separates the operations in the time domain, by preforming the uplink and the downlink in separated periods. This method requires a greater synchronism compared to the FDD and doesn't allow the uplink and the downlink to occur simultaneously[43].

Without Channel Side Information

When there is no possibility of obtaining CSI, Space-Time Block Codes (STBC), are the most used strategy to exploit transmit diversity. To fully benefit from transmit diversity, when implementing STBC we usually assume that there is total knowledge of the channels, at the receiver's side, and that each data stream is independent. An efficient method of obtaining transmit diversity without CSI, can be achieved by implementing the Alamouti space-time code. This code begins by taking two symbols of a digitally modulated data stream, as depicted on figure 2.7 The symbols, s_1 and s_2, are then processed by a block that implements the following matrix:

$$\begin{pmatrix} s_1 & -{s_2}^* \\ s_2 & {s_1}^* \end{pmatrix} \tag{2.8}$$

each column of the matrix represents a different time instant and each line represents the information to each antenna. This way, at the first instant the antenna one will transmit the symbol s_1 and the second antenna the symbol s_2, continuing this logic, at the second instant

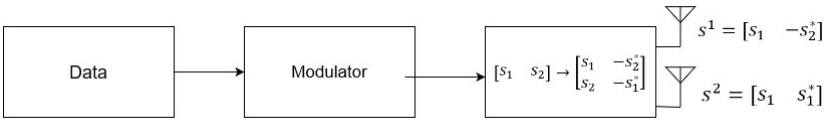

Figure 2.7: Alamouti Scheme.

the first antenna will transmit $-s_2^*$ and the second s_1^*. The data vectors for the first and second antenna are given respectively as:

$$\begin{bmatrix} \mathbf{s_1} & -\mathbf{s_2}^* \\ \mathbf{s_2} & \mathbf{s_1}^* \end{bmatrix} \tag{2.9}$$

Looking at the vectors we can conclude that they are orthogonal to each other, hence to the receiver these are two orthogonal streams with different channel properties, thus achieving a transmit diversity of two. The Alamouti scheme was the base code for many other space-time codes [44][45][46], besides, it is a very popular as it can be implemented with low complexity decoders, it doesn't require CSI to obtain full transmit diversity. This coding was used on LTE due to its performance on dual transmit antenna and also for its simplicity to incorporate on existing systems without completely redesigning them[36].

2.3 Conventional Cellular Architecture

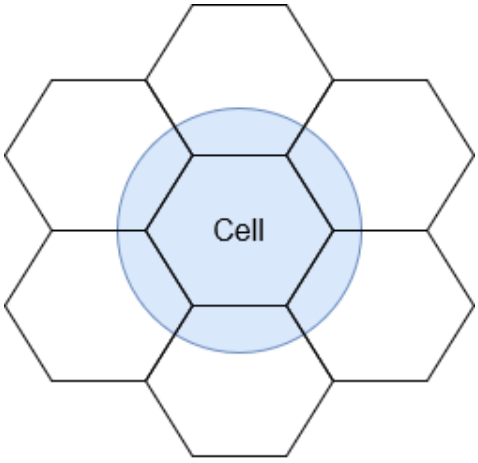

Figure 2.8: Honeycomb cell pattern.

Most of the cellular networks are divided in multiple macro-cells with a roughly hexagonal shape. The radius of each cell depends on its area of deployment, and may vary between 500m, in the cities, and 30km in rural areas. The access point in these is granted by a single Base Station (BS) that covers the entire area. The BS does all the downlink and uplink operations

and can be consider as a Broadcast Channel, for its use as a transmitter to several receivers, and also as a multiple access point, for its use as a receiver for several transmitters. These networks are usually structured like a honeycomb pattern as seen on figure 2.8. Because of how close the cells are to each other, their deployment is carefully planned both to maximize their coverage and to minimize the Intercell Interference (ICI) as all base stations transmit on the same frequency band and with the same power level, around 5 to 40W[24].

To minimize ICI without sacrificing completely the spectrum efficiency, a concept of Frequency Reuse (FR), is implemented[47]. The FR consists in using a set of different frequencies in a cluster of adjacent cells and reusing them when there is enough distance to mitigate ICI. Represented in figure 2.9, we can see that there are three different sets of frequency channels, that are attributed to several cells while avoiding interference between them by attributing the same frequency with minimal space between the cells. This typology of the network can be called a homogeneous network, due to the nonexistent coordination between base stations, in terms of channel usage. Due to its use of static FR, where each cell is allocated as a set of frequencies, there is always an inevitably waste of radio resources for its inefficient use of the frequency spectrum. Besides, this system may suffer from a low data rate problem, as the load data traffic is not the same in every cell, a cell that as a greater demand for traffic may not be able to manage it due to its limited number of set frequencies.

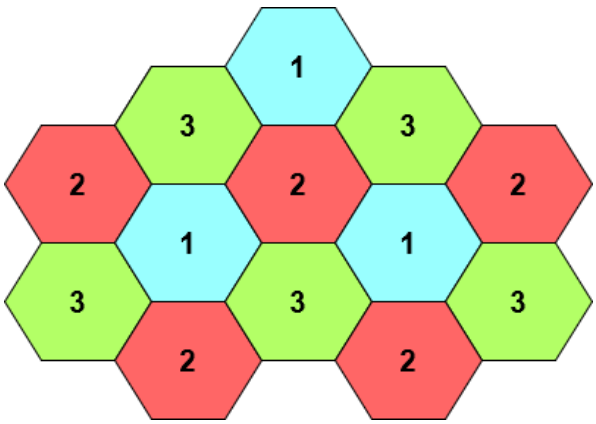

Figure 2.9: Frequency reuse system.

Even though there are some networks that use dynamic frequency planning, that may allow the allocation of frequencies according to the cells traffic demand or its interference measurement, these systems are not flexible and fast enough to mitigate the waste and the starvation of the radio resources. It is expected that the 5G will bring a new concept of a network called HetNet, where the increase of the number of access points allied with better coordination between them, will allow for greater data traffic while still achieving better use of the frequency spectrum

2.4 Heterogeneous Network

With the increase of the traffic demand and because of the optimization plateau reached by the transmission bases, the homogeneous network structure is becoming obsolete [48] [24]. In dense urban areas where the number of terminals is high, it is difficult to provide the same QoS to all users within the same cell, besides, it has become difficult to obtain new sites to install big BS in these urban areas. To reply to the expected demand of traffic data, and as the single cellular transmission points have evolved into a point nearly optimal, to what has been theorized in terms of information capacity limits, resorting to another network topology for 5G may be one of the answers to the expectations of this new generation [24]. A heterogeneous network, HetNet , opposite to the homogeneous network, proposes to increase the number of access points on a macro-cell by deploying, in a roughly unplanned manner, femto and pico-cells alongside relay base stations, that are much cheaper, smaller and easier to install, unlike their macro-cell counterparts[22][23]. All these different technologies are to coexist in the same cell without interfering with each other, nor the main base-station.

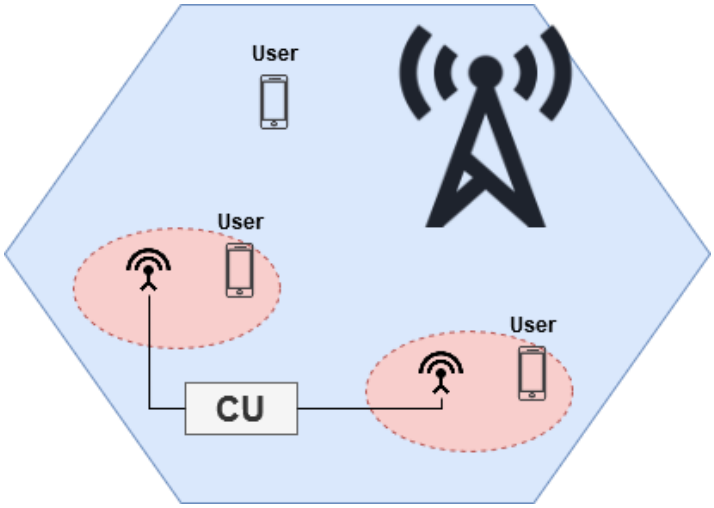

Figure 2.10: Heterogeneous network.

Contrary to the high-power transmissions of the BS, these small cells will transmit with much lower power and they will be scattered by the entire macro-cell, eliminating coverage holes, relieving the traffic load in hotspots, and providing a much more dedicated service to the users connected to them[22][23]. The HetNets are not an entirely new concept, as its implementation has been studied and proposed to boost coverage range and help with the traffic grow on former technologies such as 3GPP LTE and LTE-A, presenting positive results on both objectives and technologies[49] [24]. With the expansion of access points, one of the biggest challenges in the implementation of this network system comes with the interference management, as the interference can be cross-tier, between small cells and the macro-cells, and co-tier, between the small-cells from the same tier. To solve this problem, it is imperative to

use Advanced Interference Management techniques to coordinate the transmissions and allow better management of time, frequency, and spatial resources. The method used depends on the network interface in which these would be applied. For example, on an LTE-A interface, that uses OFDM, some studies have proven that a management technique as Fractional Frequency Reuse (FFR) is effective since this technology tries to increase the frequency spectrum efficiency by using carriers separated by a small factor[50] [51]. The performance of the HetNets depends mostly on its capacity in managing the existing RF resources and the mitigation of interference between cells by applying interference management techniques.

2.4.1 Femto-cell

Femto-cells popularity has been growing over the years for their flexible and low-cost deployment, also for their potential in reducing the overall network cost compared to a pure macro-cellular structure [52], and because of their applicability to achieve the data rates and network capacity improvements that are expected on 5G. Several technical studies were done to evaluate the performance of the femto-cells associated with different technologies. Such as the GSM used on 2G, the HSPA, in 3G, LTE, and LTE-A[53][49]. These cells are meant to be used as an indoor access point that can be installed by the end-user, in an unplanned manner, just like a router nowadays, and they ought to use the Digital Subscriber Line (DSL) or the modem cable as a backhaul[24]. With transmission powers of around 100mW, the coverage area of these cells is very limited, making them perfect for small areas like households, offices, and subways. Femto-cells access mode can be classified as open, where any terminal can be connected to it, closed, when the access is restricted to a limited number of users, and finally hybrid, in which it is used a priority system that gives preference to the cell subscribers over users that do not belong to the subscriber's group.

2.4.2 Pico-cell

Pico-cells are similar to macro-cell base stations, but with transmissions with a power range of 250mW to nearly 2W. Their stations are normally equipped with omnidirectional antennas with a 5dBi gain and they are usually used to cover areas from 40 to 75m of diameter. These cells are to be used on hotspots like airports and shopping centers, so they are deployed in a planned manner to cover the needed hot spots, contrary to the femto-cells[50].

2.4.3 Relay Base Station

A Relay base station, also known as Relay Nodes (RN), uses a transmission power of around 250mW to nearly 2W, just like the pico-cell, but with the singularity of not using a physical backhaul connection with the rest of the network. These cells are to be deployed in areas where a physical connection with the rest of the network is too difficult. The backhauling

of these stations is done via a wireless connection, this connection can be done using the same frequencies as the communications to the users, these stations are known as in-band relays, or in a different and dedicated frequency, out-of-band relays[24].

2.4.4 Backhauling

Backhaul is the link that connects the transmission bases to each other within a macro-cell, establishing the base infrastructure of the wireless network. The backhauling link can either be physical or wireless and they are used by the various base stations to communicate with each other and to the backhaul network core. The cost and the quality of these connections may vary from a high-speed optical fiber or dedicated Line of Sight (LOS) microwave, to a slower DSL or non-LOS microwave[49]. The type of connection is related to the type of cell and its location. For example, a femto-cell inside a household would use the DSL as the backhaul link, while a pico-cell in a train station would use a LOS microwave link. Backhauling is a determinate factor for HetNets, as it allows the coordination of the different cell transmissions and also the management of the different RF resources, giving more flexibility to the entire system in terms of Interference Management between cells. The design of the backhaul network for the HetNets will be very challenging, due to the expected diversity and the number of small-cells that are to be deployed. For this reason, the network as to be carefully planned to guarantee the same QoS depending on the cell and its backhaul link.

2.4.5 Interference Mitigations Techniques

It is expected that 5G will suffer more from ICI than any other cellular network generation, due to the high deployment of femto and pico-cells to establish heterogeneous networks, HetNets. As stated before, this network typology will demand greater coordination between access points, as these are to coexist in a single macro-cell, besides, due to the ad hoc deployment of femto-cells, ICI is nearly inevitable[54][55]. Although ICI mitigation is a critical point on 5G, interference management techniques are not a new concept. The implementation and studies of interference management have been developed through the decades according to the needs of each cellular generation [54] [50].

The 2G, which was primarily designed to voice services, that do not require a lot of the frequency spectrum, was implemented on a homogeneous topology network scheme. As the cell planning for 2G is quite regular, it used FR. Schemes to mitigate the ICI between its cells.

With the general use of CDMA on the 3G, the interference among mobile stations increased since the FR factor for CDMA is one. Thus, power control techniques were mostly used, as most of the interference was related to the emitted power, especially at the cell-edge.

The 4G brought the wide use of OFDM in order to achieve greater data rates while still maintaining efficient use of the spectrum. This also brought the use of techniques like FFR, to better coordinate interference in the frequency-domain.

The main idea of FFR is to divide each macro-cell into spatial areas, as represented on figure 2.11 To each of these areas it is assigned a different frequency sub-band. With this division, communications devices at the cell-edge do not interfere with those in the center-zone. Allying this spatial division with a proper allocation of different channels to the edges of the adjacent cell, it is also possible to mitigate ICI[50].

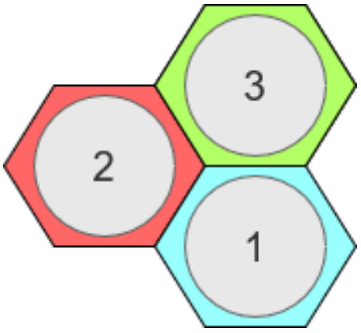

Figure 2.11: Fractional frequency reuse system.

With the 4G also came the first deployments of femto-cells, to help the base stations with the data traffic in hotspots such as malls and sports stadiums, hence becoming the first HetNets. The deployment of these small cells also introduced a new ICI that occurred between the base stations of the macro-cells and the femto-cells, that was different from the ICI of the former generations. The interference in this kind of network is mostly due to the transmission of the base stations, so much that these can be considered as the dominant source of interference. To mitigate this kind of interference the concept of enhanced Inter-Cell Interference Coordination began to be developed and introduced techniques such as Almost Blank Subframes (ABS), and Coordinated Multi-Point (CoMP)[56][54].

The ABS can be defined as a minimum transmission subframe in the time domain, in which the base stations, that are the dominant interferer, won't transmit any data during the period of time of the subframe stream beside the Common Reference Signals (CRS), to provide information support to the rest of the network. An example of an ABS frame is depicted in figure 2.12. The entire cell access points work in a coordinated and synchronized manner according to the ABS patterns.The ABS patterns are configured according to the information that the macro cell receives from the small cells. The macro-cell then decides which subframes are to be set as ABS and transmits it to the rest of the cells[57].

The CoMP was developed particularly to improve the QoS to users that receive signals from different cells. CoMP requires a great amount of coordination and information sharing between cells, as it uses multiple antennas, that may or may not be from the same cell, to do the downlink and uplink operations. By exploiting multiple antennas from different cells, CoMP is able to take advantage of multiple transmission techniques such as Coordinated Beam-Switching and Coordinated Scheduling, where the user information would only be used

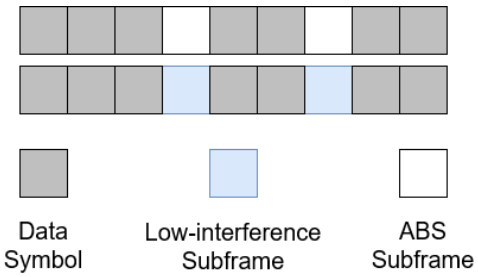

Figure 2.12: ABS frames.

at the serving cell, but still needs coordination between all interfering cells[58]. Although its versatility on applicable techniques, CoMP is difficult to implement, due to its requirements on backhaul transmission capability and the complexity of joint processing. Due to its complexity CoMP is mostly used on necessary control signals.

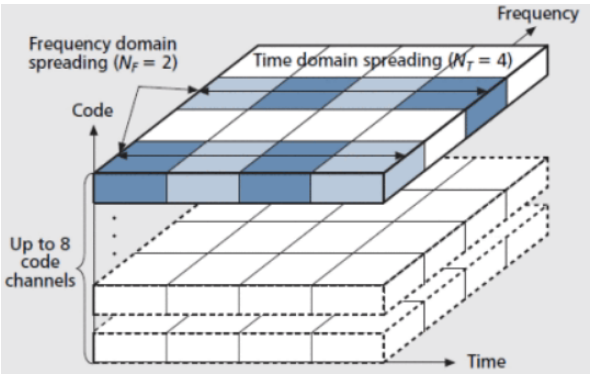

Figure 2.13: OFCDM frames[59].

5G will take advantage of an ah doc deployment of small cells to offload the base stations and enable a more dedicated service to the users. This will result in an ICI with no precedence as these cells will suffer from a two-tier interference, co-tier, between the same kind of cells, and inter-tier, between cells of different sizes. Hence the previous techniques developed for the former generations, will not be enough to mitigate all the interference that is expected to exist. One of the suggestions to mitigate ICI on 5G, maybe a more generalized implementation of CoMP alongside Super Base Stations[60] with a high computer and storage capability. These new BSs are to be deployed with the objective of processing information from several cells, that are connected to the Super BS via fiber or high-speed wireless links. By facilitating more backhaul links between cells, the transfer of CSI becomes easier, allowing for the synchronism and coordination needed between cells for the CoMP to work. Another solution may be the optimization of the overall signal modulation, by switching from the LTE standard OFDM and SC-OFDM to Orthogonal Frequency and Code Division Multiplexing (OFCDM), for example[61]. The big difference between OFCDM and the former modulations is that, besides

multiplexing the symbols by different frequencies and time frames, it will also be dividing them by spreading codes. It has been shown that OFCDM can provide a 1.6dB gain over the OFDM, besides mitigating the ICI.

Another candidate might be Interference Alignment (IA). Recent studies have shown that in wireless interference channels, users are able to get half of the channel capacity free from interfering signal at a high SNR [62]. As this thesis main theme is about an IA ICI mitigation method, an entire section will be dedicated to IA.

2.5 Interference Alignment

Interference can be a critical problem when trying to establish reliable communications in a multi-user wireless network, as these networks are very susceptible to suffer from interference, not only because of the overlapping nature of its transmission channels but also due to the broadcasting and multi-access requirements of a wireless network [42]. As stated before, interference in wireless communications is expected to grow even more with the 5G, especially due to the expected exponential deployment of access points in order to build the structure for the HetNets. Interference Alignment has become a promising contestant to tackle this future problem, as it has been shown theoretically to be the best approach in terms of channel capacity and Degrees of Freedom (DoFs). DoFs can also be referred to as multiplexing gain. IA requires a high SNR level, to achieve DoFs while still being able to fully mitigate the ICI [62]. IA can be obtained in space, time and frequency domain, but due to the predominant use of MIMO systems in the last decades and also with the arrival of massive MIMO with the 5G, most of the development and studies on this interference management technique are in the space domain. The basic concept of IA, when applying it in the space domain, is to use precoders on the transmitters in order to send the data stream with an assigned directional vector. Then at the receiver end, the interfering signals can be aligned and canceled with a decoding matrix that is orthogonal to the directional vector of the incoming signal, allowing for an interference-free reception of the intended signal. If we assume the K-user interference channel system presented in [62], independently of the number of interfering transmitted signals, each receiver will align all the incoming unwanted signals to one half of its space, while saving its other half completely free for the desired signal. This way, IA maximizes the number of different signals being transmitted simultaneously, hence achieving more DoFs (multiplexing gain). To accurately eliminate the interference between users, each node of a MIMO IA network must have an adequate number of antennas, this number can be determined by its feasibility condition [63]. Although being a promising solution for future interference problems, IA has some challenges in its practical implementation that must be tackled first before being widely used. One of the challenges comes with its reliability on CSI in order to calculate the ideal directional vectors for the transmitters and decoding matrices at the

receivers. As CSI is usually calculated at the receivers and only then transmitted to the transmitter via a backhaul link, IA may have problems when dealing with high-mobility and fast-fading system, due to the overhead CSI acquisition. Besides, IA also depends on a high SNR to maintain its theorize performance, this can be a great weakness when dealing with badly conditioned channels or when SNR is low. More issues with its implementation care further explained in [64].

The Three-User IA structure

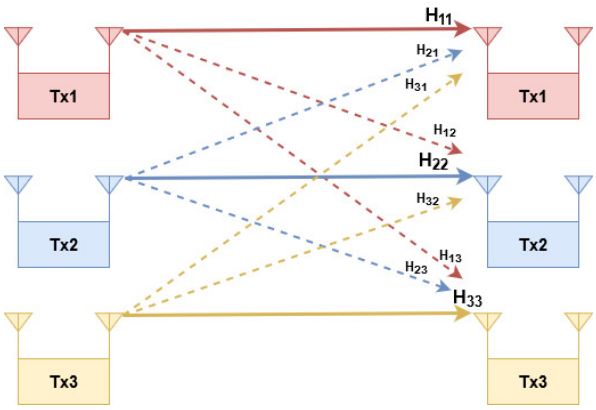

Figure 2.14: Three users system.

To further understand the concept of IA applied to a MIMO network, we will consider the system represented on figure 2.14 Let us assume that each transmitter k is set to transmit a symbol x_k to its corresponding receiver j, where the number of transmitters is equal to the number of receivers, three. The symbols are then coded using a directional vector v before being transmitted via the interfered channels, that are represented by the matrix H_{kj}. Hence the received signal at the j^{th} user can be given by:

$$y_{j,j} = H_{j,j}v_j x_j + \sum_{j \neq k} H_{j,k}v_k x_k + n_j, \tag{2.10}$$

where n_j is the noise observed at the receiver j. In a MIMO system with N transmit antennas and M receive antennas, H_{kj} has N×M dimensions. In this case, $\mathbf{H}$ is 6×6 as the system has three transmitters, each one equipped with two antennas, and three receivers also equipped with two antennas each. When it comes to canceling the interfering signals, independently of the size of the directional vector used on the transmitter, at the receiver must be a linear equalizer W_j that cancel all the interference it observes from the rest of the users, by accomplishing equation (2), without canceling the desired signal $H_{j,j}\ v_j\ x_j$ [64].

$$W_j(H_{j,k}v_k x_k) = 0, \forall j \uparrow k. \tag{2.11}$$

Isolating the receiving signal at Rx1,y_{11} , can be given by the following expression:

$$y_{11} = H_{11}v_1x_1 + H_{21}v_2x_2 + H_{31}v_3x_3 + n_1, \tag{2.12}$$

Furthermore, with the precoding we can consider that $H_{11}v_1 = [a, b]^T, H_{21}v_2 = \beta[c, d]^T and H_{31}v_3 = \gamma[c, d]^T$. Ignoring the additional noise, we can write the received signal from each antenna of the first receiver as:

$$y_{11} = ax_1 + c(\beta x_2 + \gamma x_3) \tag{2.13}$$

$$y_{11} = ax_1 + d(\beta x_2 + \gamma x_3) \tag{2.14}$$

As the signals coming from the Tx2 and Tx3 are to be aligned at the receiver, through a proper equalizer designed to achieve IA, we can assume $x_4 = (\beta x_1 + \gamma x_3)$. We can then write the previous equations:

$$y_{11} = ax_1 + cx_4 \tag{2.15}$$

$$y_{11} = ax_1 + dx_4 \tag{2.16}$$

As the number of equations is equal to the number of variables, the intended symbol can be recovered. The DoFs, in this example, are three and is equal to the number of streams that can be transmitted free of interference. The performance and the DoFs achieved be IA are directly connected to the number of time frames, frequency blocks and antennas available for the precoding. Besides, this interference management technique requires a feasibility Condition in order to be successful [65].

Feasibility Condition and Performance Metrics

To fully work, IA needs enough antennas at its transceivers to achieve its purpose. The ideal number of antennas can be determined by the feasibility condition. The feasibility condition is used to determine the solvability of the polynomial equations obtained on the IA system, as represented in. Basically this condition is used to prove that the equations are only solvable if the number of variables is not less than the number of equations [63]. It has been proven that IA is feasible if the number of antennas used can satisfy the following condition [66].

$$N \geqslant \frac{d(K+1)}{2} \tag{2.17}$$

Where N, represents the total number of antennas to be used, K represents the total number of pairs of antennas and d represents the DOFs that we want set on the system. Hence, from the equationequation (2.17) it has been demonstrated that the total DoFs of an IA system can be given by:

$$d \geqslant \frac{K(M+N)}{K+1} \tag{2.18}$$

Where d are the DoFs intended for the system, K represents the transmitter-receiver pairs, M is the number of antennas on each transmitter and N the number of antennas on each receiver. In most cases, these are the equations to be considered when designing a proper IA system.

When it comes to measuring the performance of an IA system, DoFs are one of the most important aspects to study [67]. The DoFs are usually represented by η and can be determined as

$$\eta = \lim_{\rho \to \infty} \frac{C(\rho)}{\log_2 \rho} \tag{2.19}$$

Where C represents the sum capacity of the network, and ρ is the SNR. The previous equation can also be written as

$$C(\rho) = \eta \log_2 \rho + o(\log_2 \rho) \tag{2.20}$$

where EQ represents the Additive white Gaussian noise (AWGN), while η (DoFs) represents the number of signals without interference when SNR meets the infinity, this can also be referred to as the capacity pre-log factor. Thus, the DoFs are equal to the number of interference-free data streams that are transmitted in an IA system [68]. Although DoFs is widely used as a metric of the available signals in IA networks, some more practical measures of performance have been adopted in more recent studies [69] [70], such as the sum rate, that measures the spectrum efficiency, the BER and outage probability, that measures the received signal quality [68].

2.5.1 Interference Alignment for MIMO HetNets

As discussed before, HetNets are a strong contestant to solve rapid increase of traffic demand in wireless networks [71][72][73]. By deploying SCs in conventional macro cellular networks, both the indoor and hotspot coverage is improved, besides, the network capacity will also be increased because of the higher spatial properties of the system. Although its qualities, HetNets also bring severe interference with its massive deployment of small cells. As stated before, interference in these cooperative networks can be categorized into two categories, cross-tier, and co-tier interference. These two kinds of interference handicap the spatial gain brought by small cells. Thus, interference management is vital to the HetNet performance. In order to address the interference issue, many interference avoidance techniques have been proposed, such as frequency and time partitioning approaches [74][73]. However, as the trend is to increase the number of antennas on BSs and on the User equipment, interference techniques that can exploit the MIMO system properties have been gaining popularity. IA which is an advanced beamforming technique has been proposed to manage the interference in wireless networks, as it has shown effectiveness when used on conventional macro cellular networks [75][76]. However, some of the characteristics of the HetNets make IA harder to be applied, such as the different kinds of tier interference, that are more challenging compared to the conventional networks, and also the disparity between the number of small cells to the limited number of antennas on BSs and User equipment, which makes harder to achieve the IA feasible condition [63][77]. There have been several works where IA has been tested on a HetNet. For example, in [78] and [69], to cope with the co-tier interference, the SCs were divided into clusters to achieve IA. Although the interference among cells in the same cluster is canceled, the interference between different clusters was not handled.

Chapter 3

Interference Mitigation Algorithms for HetNets

In this chapter, we present interference alignment algorithms recently proposed. First, it is presented the general system model and three algorithms with different retirements in terms of channel state information feedback. Then, we describe the simplified model and algorithms to be implemented in hardware. Finally, this chapter ends with a detailed explanation of the mathematical manipulation done for hardware implementation.

3.1 General System Model

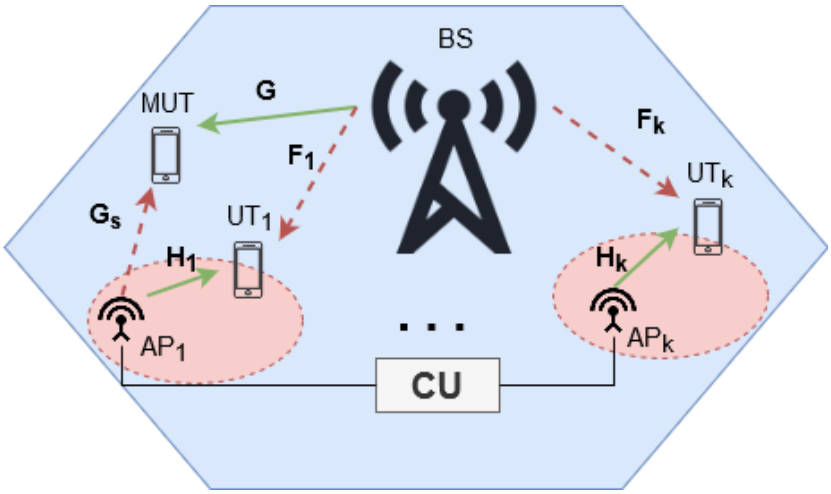

Figure 3.1: System model.

This section will introduce the proposed system model in [27] since it was the general model considered in this work. The general system model constitutes a conventional macro-cell BS, whit a set of K small-cells, overlaid on its coverage area. Additionally, there is a Macro-cell User Terminal (MUT), and small-cell User Terminals (UTs), as represented on figure 3.1. From the BS coverage perspective, the MUT can be considered as the primary user, while the UTs are the secondary users. The small-cell's Access Points (APs), are all connected to a Control Unit (CU) via dedicated backhaul links, in order to create a network capable of sharing the channels information. The BS is also linked to the CU allowing for a joint prepossessing of all transmitted signals from the access points. The small-cell secondary users, UTs, must perceive the incoming signals from the BS as interference as they can only be served by their correspondent AP. For that reason, the connection between the BS and the UTs cannot happen as illustrated on figure 3.1 by the red lines. Another key element of the system is that both the terminals and the access points are communicating on the same radiofrequency band. In this model, we will only consider the downlink transmission from the access points to the terminals, where the BS and the APs transmit with a power signal of P_m and P_s, respectively.

3.1.1 Base Station Signal Model

Both the BS and the UTs are equipped with M_m antennas while the main user, MUT, is equipped N_m, where M_m is greater than N_m. The signal transmitted by the BS, $\mathbf{x_p}$, can be expressed by:

$$\mathbf{x_p} = \gamma_m \mathbf{v_p} d_p, \tag{3.1}$$

where $\gamma_m = \left(P_m \backslash tr(\mathbf{v_p}^{\mathbf{H}} \mathbf{v_p})\right)^{\frac{1}{2}}$, $\mathbf{v_p} \in \mathbb{C}^M \times N, d_m \in \mathbb{C}^N$, denote that γ represents the power normalization constant, $\mathbf{v_p}$ is a directional vector added by the BS precoder, and d_p the transmitted data. Thus, the signal received at the MUT, $\mathbf{y_p}$, is given by

$$\mathbf{y_p} = \mathbf{G}\mathbf{x_p} + \mathbf{G_s}\mathbf{x_s} + \mathbf{n_p}, \tag{3.2}$$

where $\mathbf{G} \in \mathbb{C}^{(N_m \times M_m)}, \mathbf{x_p} \in \mathbb{C}^N, \mathbf{G_s} \in \mathbb{C}^{(N_m \times M_m K)}, \mathbf{x_s} \in \mathbb{C}_m^M, n_p \in C_m^M$, denote that $\mathbf{G}$ corresponds to the channel between the BS and the MUT, $\mathbf{x_s}$ represents the data symbols from the small-cells APs, $\mathbf{G_s}$ corresponds to the channels between the APs and the MUT, and finally $\mathbf{n_p}$ the white Gaussian noise.

3.1.2 Small-Cell Signal Model

Considering now the small cells APs and their users UTs, each AP_k is equipped with M_s antennas while each UT_k is equipped with N_s receiving antennas. The transmitted signal from each small-cell AP can then be written as

$$\mathbf{x_s} = \gamma_s \mathbf{v_s} d_s, \tag{3.3}$$

where $\gamma_s = \left(P_s \backslash tr(\mathbf{v_s}^{\mathbf{H}} \mathbf{v_s})\right)^{\frac{1}{2}}$, $v_s \in \mathbb{C}^{M_s K \times (N_s - N_m)K}, d_s \in \mathbb{C}^{(N_s - N_m)K}$, denote that γ_s represents the power normalization constant, $\mathbf{v_s}$ is the zero forcing precoder, determined at the CU, and d_s is the transmitted data. The signal received at an UT, $\mathbf{y_s}$, after passing through the filter (W_s) is given by

$$\mathbf{y_s} = \mathbf{W_s}\left(\mathbf{H_k x_s} + \mathbf{F_k x_m} + \mathbf{n_{sk}}\right), \tag{3.4}$$

where, $\mathbf{F_k} \in \mathbb{C}^{(N_s \times M_m)}, \mathbf{H_k} \in \mathbb{C}^{(N_s \times M_s K)}, n_{sk} \in \mathbb{C}_s^N$, denote that $\mathbf{F_k}$ represents the interference channel between the BS and the UTs, $\mathbf{H_k}$ is the channel between the AP_k and their correspondent UT_k and $\mathbf{n_{sk}}$ is the white Gaussian noise. We will assume that the BS does not have any information about the UTs, only the channel $\mathbf{G}$ towards MUT, thus the precoder at the macro-cell won't change because of the secondary users. Additionally, we will also consider that the UTs have channel information about $\mathbf{F_k}$ and that the CU provides to each AP the information of their desired channel $\mathbf{H_k}$.

3.1.3 Interference from Base Station towards the secondary users

As the secondary users, Uts, can be severely affected with interference from the BS, each user applies a filter matrix to the incoming signal that fulfills the following zero interference condition:

$$\mathbf{W_k F_k v_p} = 0, \tag{3.5}$$

In order to satisfy this condition, $\mathbf{W_k}$ has to be design according these expressions

$$\mathbf{W_k} = \mathbf{A}(\mathbf{F_k})^{(-\mathbf{1})}, \tag{3.6}$$

$$\mathbf{A} = \mathbf{null}(\mathbf{v_p})^{\mathbf{H}}, \tag{3.7}$$

where $\mathbf{A}$ is the alignment direction, that, as denoted on the previous equation, must be designed according to the directional vector $\mathbf{v_p}$. As mentioned before, $\mathbf{v_p}$ is a vector implemented at the BS precoder prior to its signals transmission. The alignment direction, $\mathbf{A}$, may or not be designed with the information shared from the BS to small-cells through the CU network. When $\mathbf{A}$ is created with the channel information at the APs, the small-cells can align their transmission accordingly so that the received signal at the UTs is free of interference. The alignment direction also specifies the interference transmissions from the BS towards the UTs. In the following subsections, three different methods of determining $\mathbf{A}$ will be present, that vary on their feedback on channel sate information requirements.

Static Method

In this method, it is assumed that the precoder at the BS is fixed and it will never change its value. Therefore, it is also assumed that the value of the precoder is known at the UTs. For example, the precoder at the macro cell could be a vector such as, $\mathbf{v_p} = [\mathbf{1}\ ,\ \mathbf{1}]^{\mathbf{H}}$, whereas $\mathbf{A}$ would be a vector as

$$\mathbf{A} = [\mathbf{1}\ ,\ \text{-}\ \mathbf{1}] \tag{3.8}$$

thus, this method needs no feedback link as both the precoder and the alignment direction are static and do not require channel information, making it also the least robust from all three schemes. However, this will be the method that will be put to test in this work.

Coordinated Method

Unlike the previous method, in the Coordinated method, the alignment direction is designed according to the CSI from the BS about its channel $\mathbf{G}$ with the MUT. This method requires the most CSI, as the coordination between the BS and the APs depends totally on the knowledge of $\mathbf{G}$ channel state. The full coordinated method is also the most robust of the three. If we consider a BS equipped with more than one antenna and using a zero force precoder, we should use these conditions

$$\mathbf{v_p} = \mathbf{G^H}(\mathbf{GG^H})^{-\mathbf{1}}, \tag{3.9}$$

$$\mathbf{A} = \mathbf{null}(\mathbf{v_p})^{\mathbf{H}}. \tag{3.10}$$

Two-bit Method

The two-bit method tries to achieve a balance between the feedback requirements and performance, compared to the two schemes previously mentioned. This method requires CSI as it uses the same precoder as the full coordinated scheme, however, the alignment direction at the receivers only requires the sign of directional vector $\mathbf{v_p}$ for its design. Hence, to apply this scheme the following conditions are used

$$\mathbf{v_p} = \mathbf{G^H}(\mathbf{GG^H})^{-\mathbf{1}}, \tag{3.11}$$

$$\mathbf{A} = \mathbf{null}(\mathbf{sign}(\mathbf{v_p}))^{\mathbf{H}}. \tag{3.12}$$

As the feedback requirements for the two-bit are not as great as the full coordinated, the performance of the scheme is also a bit lower. Nevertheless, the two-bit method does not require a backhaul link as expensive and robust as its counterpart, thus achieving a balance between price and performance.

The following figure depicts the difference between the BER performance from the connection between the BS and the MUT for each method while varying the SNR levels.

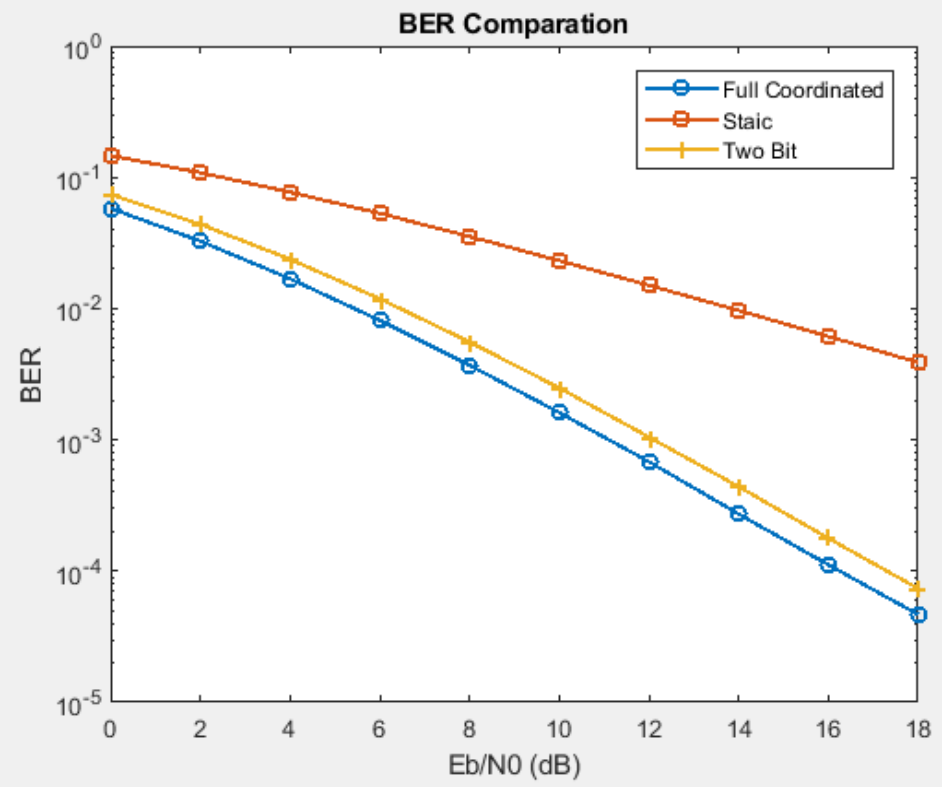

Figure 3.2: BER performance of the different methods.

3.2 Simplified System Model

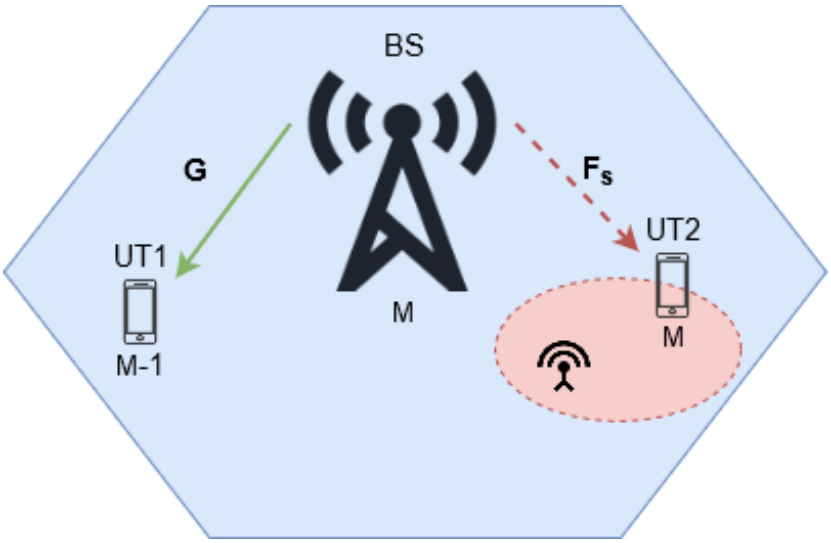

Figure 3.3: Simplified System model.

In this section we will describe the simplified scenario considered for hardware implementation. We consider only the interference that the BS may cause to the secondary users. For simplicity propose, the interference that the small-cells may cause to the primary user is not considered in this work, as well as its transmissions towards their secondary users. The aim is to implement an interference mitigation algorithm that removes the interference that the BS causes to the secondary users, and at the same time, allows the data to be successfully transmitted from the BS to primary users. Thus, the main objective of this dissertation is to implement both the equalizer of the MUT and filter of the UTs, while considering the downlink scenario from the macro-cell BS. Therefore, in the implementation it is only considered the following elements of the system model of section 3.1: the conventional BS, the MUT and a single small-cell user terminal, UT. The reason why it is only consider a single secondary user, UT, it is because all the UTs are supposed to use the same filter design for interference mitigation, thus considering more than one secondary user would lead to the same results. To simplify the description of the method used, the main terminal user will now be referred to as UT1 and the single small-cell user terminal will be referred to as UT2, as represented on figure 3.3. Both the BS and UT2 are equipped with the same number of antennas M, where M=2. The main user UT1 is equipped with M-1 antennas, in this case, a single antenna. In our model, we will consider that the only transmitting device is the BS, whereas the users will only work as receivers. The base station, BS, must only establish a viable downlink connection to its main user, UT1. This connection can be seen on figure 3.3 with **G**, in green, that represents the transmission channel. As explained on section 3.1, UT2 must perceive the incoming signals from the BS as interference. The channel between the BS

and the UT2 is illustrated on figure 3.3 by **F**, in red. For the scope of this thesis, it was only implemented the static method, previously presented in section 3.1.3.

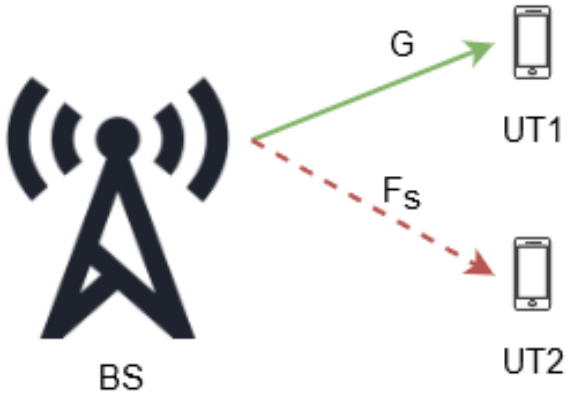

Figure 3.4: System model signals.

3.2.1 Static Method

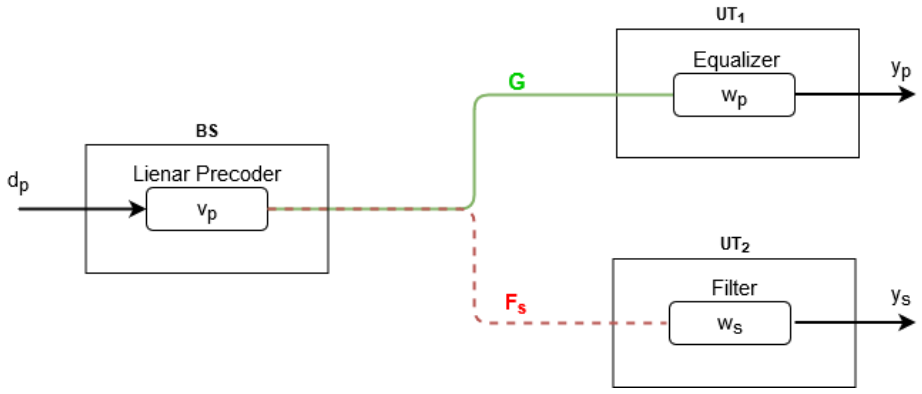

Figure 3.5: Static Method precoder and filter.

The implementation of the static method represented on figure 3.5, begins with a precoder on the transmitter that will apply a directional vector, $\mathbf{v_p}$, to the symbol that is going to be transmitted d_p. This signal travels through the channels $\mathbf{G}$ and $\mathbf{F_s}$. We assume that the UT1 as no information relatively to UT2, thus its equalizer, $\mathbf{W_p}$, is static and will not change with time and can be given by:

$$\mathbf{W_p} = (\mathbf{G v_p})^{\mathbf{H}}. \tag{3.13}$$

We will also assume that the BS does not have any information about the UT2, hence the precoder at the transmitter is fixed and does not change because of the second user. As the UT2 can be severely affected with interference from the BS, a filter matrix is applied to the incoming signal to fulfill the following zero interference condition

$$\mathbf{W_p F_s x_p} = \mathbf{0}. \tag{3.14}$$

To satisfy the previous condition, $\mathbf{W_s}$ must be design according to an alignment direction vector $\mathbf{v}$, that is correlated with the directional vector $\mathbf{v_p}$, at the precoder. These two need to be orthogonal so that the filter $\mathbf{W_s}$ can easily remove the interfering signal from the BS. Both $\mathbf{W_s}$ and $\mathbf{v}$ can be respectively expressed as

$$\mathbf{W_s} = \mathbf{v}(\mathbf{F_s^{-1}}) \tag{3.15}$$

$$\mathbf{v} = \mathbf{null}(\mathbf{v_p^H}) \tag{3.16}$$

Analyzing the signal at the UT2, the orthogonality between vectors removes the interference. Thus, we can write the signal at the secondary user as

$$\mathbf{v}(\mathbf{F_s^{(-1)}})\mathbf{F_s v_p d_p} = \mathbf{0}. \tag{3.17}$$

As we are going to use the static method, the alignment direction is static throughout the entire time as there is no coordination or feedback information between the devices. Thus, we only need to fulfill the relation at equation (3.16) between the precoder and the filter vectors to implement the IA static method. To simplify its implementation, we are going to use a directional vector $\mathbf{v_p} = [\mathbf{1}, \mathbf{1}]^{\mathbf{H}}$, hence our alignment direction is given by

$$\mathbf{v} = [1, -1]. \tag{3.18}$$

3.2.2 UT1 Signal manipulation

Although in theory the static method seems simple, its real implementation requires some attention, as mathematical manipulations are not straightforward when designed for a hardware application. Due to this factor, both this section and the following one, are going to be dedicated to the mathematical analysis of the operations required.

As shown on the previous section 3.2.1, the main receiver, UT1, implements the equalizer $\mathbf{W_p}$, as presented in equation (3.13). Let us begin by analyzing and rewriting the received signal at UT1, expressed at equation (3.2). When ignoring the existence of noise and also assuming that the received symbol already as the channel's properties, and therefore, rewrite $\mathbf{G x_p}$ as $\mathbf{x_{p,G}}$. The received signal $\mathbf{y_p}$ can be simplified to

$$\mathbf{y_p} = \mathbf{W_p x_{p,G}} \tag{3.19}$$

By decomposing the equalizer $\mathbf{W_p}$, according to the channel disposition and assuming the

direction vector $\mathbf{vp} = [\ \mathbf{1} \quad \mathbf{1}\ ]$ we have

$$\mathbf{y_p}=\left(\begin{bmatrix} \mathbf{g_1} & \mathbf{g_2} \end{bmatrix}\begin{bmatrix} \mathbf{1} \\ \mathbf{1} \end{bmatrix}\right)^{\mathbf{H}}\mathbf{x_{pG}} \tag{3.20}$$

Each member of the channel $\mathbf{G}$ vector is a complex number, thus the previous equation can be written as

$$\mathbf{y_p}=\left(\begin{bmatrix} (\mathbf{I_{g_1}}+\mathbf{Q_{g_1}}) & (\mathbf{I_{g_2}}+\mathbf{Q_{g_2}}) \end{bmatrix}\begin{bmatrix} \mathbf{1} \\ \mathbf{1} \end{bmatrix}\right)^{\mathbf{H}}\mathbf{x_{pG}} \tag{3.21}$$

where $\mathbf{I}$ represents the in-phase value of the channel element and $\mathbf{Q}$ the quadrature values. Then, by multiplying both matrices and doing the sum of the channel's values, we get

$$\mathbf{y_p}=(\mathbf{I_{g_1+g_2}}+\mathbf{Q_{g_1+g_2}})^{\mathbf{H}}\mathbf{x_{pG}}. \tag{3.22}$$

Subsequently, the Hermitian operation is done by changing $\mathbf{Q_{g_1+g_2}}$signal. Finally, by applying the distributive property to $\mathbf{x_{p,G}}$, which can also be represented by its in-phase and quadrature values, the original signal is recovered. The cartesian representation of the signal, post equalization, is given by

$$\mathbf{y_p}= \mathbf{Re}\left(\mathbf{I_{g_1+g_2}I_{x_{pG}}}- \mathbf{Q_{g_1+g_2}}\ \mathbf{Q_{x_{pG}}}\right)+\mathbf{Im}\left(\ \mathbf{I_{g_1+g_2}Q_{x_{pG}}}- \mathbf{Q_{g_1+g_2}I_{x_{pG}}}\right)\ . \tag{3.23}$$

3.2.3 UT2 Signal manipulation

Similar to the analysis done to UT1, we will analyze the mathematical manipulations performed to create and implement the filter $\mathbf{W_s}$, as expressed in equation (3.15). First, let us simplify the received signal equation at equation (3.4), by rewriting it without the additional noise, and also switching both the channel gains and the data symbols from $\mathbf{F_s x_p}$ to $\mathbf{x_{p,F}}$, resulting in

$$\mathbf{y_s}= \mathbf{v}(\mathbf{F_s^{-1}})\mathbf{x_{p,F}} \tag{3.24}$$

Now, focusing more on the filter creation. Using the direction alignment vector $\mathbf{v} = [\ \mathbf{1} \quad \mathbf{-1}\ ]$, and rewriting $\mathbf{F_s}$ in its matrix form we have

$$\mathbf{W_s} = [\ \mathbf{1} \quad \mathbf{-1}\ ]\begin{bmatrix} \mathbf{F_{11}} & \mathbf{F_{12}} \\ \mathbf{F_{21}} & \mathbf{F_{22}} \end{bmatrix}^{-1} \tag{3.25}$$

where, as similar to the channel $\mathbf{G}$ in UT1, each element of the $\mathbf{F_s}$ matrix has its own imaginary and real part. The first operation to be fulfilled is the matrix inversion, which can be done by applying the following property

$$\mathbf{A} = \begin{pmatrix} \mathbf{a_{11}} & \mathbf{a_{12}} \\ \mathbf{a_{21}} & \mathbf{a_{22}} \end{pmatrix} \tag{3.26}$$

$$\mathbf{A}^{1} = \frac{\begin{pmatrix} \mathbf{a_{22}} & \mathbf{-a_{12}} \\ \mathbf{-a_{21}} & \mathbf{a}_{11} \end{pmatrix}}{|\mathbf{A}|} \tag{3.27}$$

After inverting the matrix and applying the matrix multiplication between $\mathbf{F_s^{-1}}$ and the vector $\mathbf{v}$, $\mathbf{W_s}$ can be expressed as

$$\mathbf{W_s} = [\ \mathbf{F_{11}} - \mathbf{F_{21}} \quad \mathbf{F_{12}} - \mathbf{F_{22}}\ ], \tag{3.28}$$

$$\mathbf{W_s} = \begin{bmatrix} \mathbf{w_{s1}} & \mathbf{w_{s2}} \end{bmatrix} \tag{3.29}$$

Thus, the equation (3.24) of the received signal can be written as

$$\mathbf{y_s} = \begin{bmatrix} \mathbf{w_{s1}} & \mathbf{w_{s2}} \end{bmatrix} \mathbf{x_{p,F}}, \tag{3.30}$$

then, by doing the multiplication between both members, $\mathbf{y_s}$ is given by:

$$\begin{aligned} \mathbf{y_s} = \mathbf{Re}\Big(\mathbf{I_{w_{s1}} I_{x_{p,F}}} - \ \mathbf{Q_{w_{s1}}}\ \mathbf{Q_{x_{p,F}}} + \mathbf{I_{w_{s2}} I_{x_{p,F}}} - \ \mathbf{Q_{w_{s2}}}\ \mathbf{Q_{x_{p,F}}}\Big) + \\ \mathbf{Im}\Big(\mathbf{I_{w_{s2}} Q_{x_{p,F}}} - \ \mathbf{Q_{w_{s2}} I_{x_{p,F}}} + \mathbf{I_{w_{s2}} Q_{x_{p,F}}} - \ \mathbf{Q_{w_{s2}} I_{x_{p,F}}}\Big)\ . \end{aligned} \tag{3.31}$$

Chapter 4

Hardware Implementation

This chapter begins by introducing the main tool used to accomplish this work, System Generator for DSP, which is a modeling tool for hardware designing. The introduction is then followed by a description of the transmitting and receiving schemes used to transmit the data signals. These two schemes establish a reliable OFDM modulated transmission between the transceivers and are the foundation of the entire design. The designs conceived for this thesis will be explained in more detail, specifically the UT1 equalizer and UT2 filter which are used to implement the proposed static method. This chapter ends with the description of the tests done to each of the created designs with their respective results.

4.0.1 Introduction to System Generator for DSP

System Generator was developed by Xilinx with the objective of creating a modeling tool for hardware designing for their own Field Programmable Gate Arrays (FPGA). This tool works as an extension of Simulink, which is a modulation and simulation tool provided by Mathlab, used to modulate various kinds of systems. Just like Simulink, System Generator simulations and models are done by designing schematics of the intended systems, using a set of blocks provided by blockset libraries.

The System Generator blockset is a library of blocks that is connected to the Simulink block editor to build functional models of dynamical systems. For system modeling, System Generator blocksets are used like any other Simulink blocksets. System Generator blocks are bit-accurate and cycle-accurate, hence they can produce values in Simulink that correspond with values produced in hardware. Every single block has its own individual documentation, with the description of each configuration and proper hardware implementation.

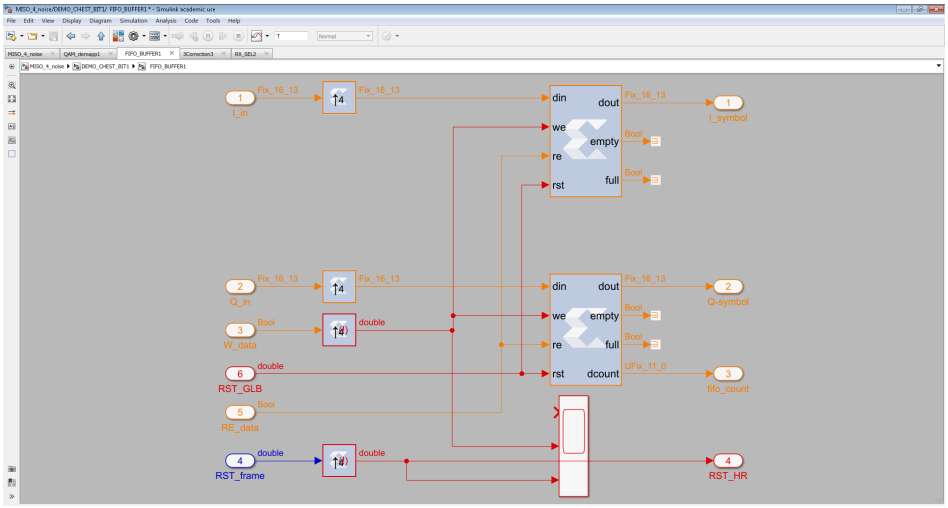

Figure 4.1: System Generator user display.

In order to provide an accurate simulation of hardware, System Generator blocks operate with three different kinds of signals, Boolean and signed or unsigned with arbitrary precision fixed-point signals. Where Boolean are represented by a single bit, whereas the other two can be represented by an arbitrary number of bits. The connection between Xilinx blocks and Simulink blocks cannot be done unconsciously, as this is only possible when using gateway blocks. As Simulink double precision continuous time signals must be sampled to be compatible to the System generator blocks, the gateway in converts the double precision signal into a Xilinx signal, and the gateway out converts a Xilinx signal into double precision. Most Xilinx blocks are capable of choosing the appropriate output types based on their input.

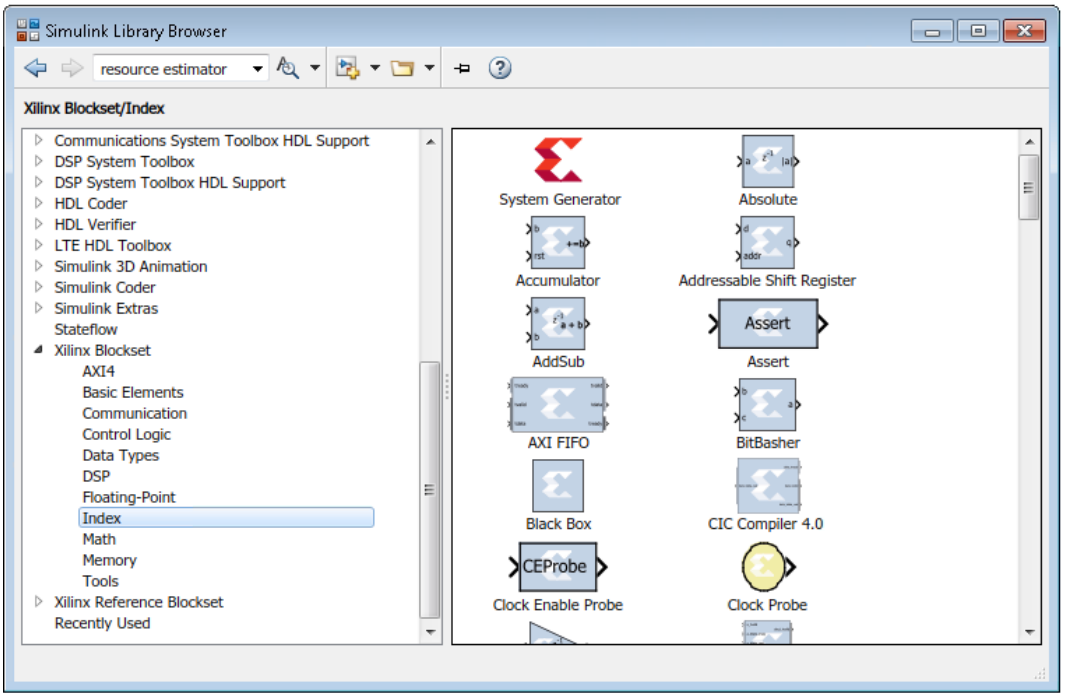

Figure 4.2: System Generator Blocksets.

Designs in System Generator are discrete time systems, therefore, the signals and the blocks that produce them have their own sample rates, excluding the need of blocks exclusively conceived for clock generation. A block's sample rate determines how often the block functions. System Generator sets most sample rates automatically. A few blocks, however, set sample rates explicitly or implicitly. An example of the blocks sampling behavior can be done by implementing the scheme depicted on figure 4.3. Where is represented a gateway that is driven by a Simulink sine wave block source and a second gateway that drives a Simulink scope. The Gateway In block is configured with a sample period of one second, while the Gateway Out block converts the Xilinx fixed-point signal back to a double as it was originally generated in Simulink but does not alter sample rates. The scope graph shows both the unaltered and sampled versions of the sine wave.

The schematic and block structure of System Generator is its greatest advantage, as it enables the design and testing of possible hardware implementations, while exploiting both Simulink's simulation and compilation speed, as well as its clean display. Besides, as it automatically generates Hardware Description Language (HDL) code from its designs, it allows users to program and implement schemes on hardware without possessing a deep knowledge on FPGAs nor HDLs, while still providing reliable results that match the ones obtained via hardware testing.

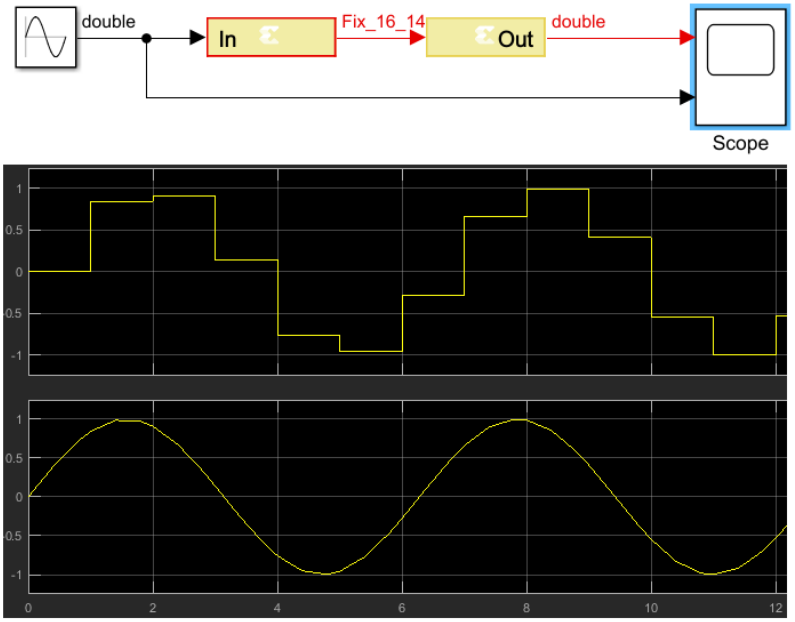

Figure 4.3: System Generator sampling rate example.

4.1 System Generator Model

In this section, we will introduce the main blocks used on this thesis work. In the interest of providing a comprehensive understanding of the implemented scheme, a subsection will be dedicated to each device. This section begins with the analyses of the transmitter and then the receivers corresponding to UT1 and UT2, respectively. The explanation will provide more detail on the blocks that were specifically developed for this project, while only roughly explaining the overall transmission and reception schemes used.

4.1.1 Transmitter

To implement the base station, we used a QPSK OFDM transmitter. As seen on figure 4.5, the system consists of a random data generation block, a block to assemble an OFDM symbol by multiplexing different types of carriers, an OFDM modulator (IFFT), and finally a buffer to assure a continuous and synchronous transmission. The continuous flow of data is achieved using different rates in the signal processing data path. The generation and modulation of OFDM symbols is done at much higher rate than the rate at which they are transmitted. Because of that, the creation of OFDM symbols is performed asynchronously and it is not a continuous process. The transmitter has two inputs, one of *Data Config.* used to enable and disable the transmission of data information on data carriers and a global *Reset* to restart the transmitter to e predefined state. It is important to have the possibility to disable the transmission of data carriers in order to verify that the channel is properly estimated, during channel estimation debugging. When the *Data Config.* has a value of '0', the transmitted signal only contains pilot symbols, while data carriers are filled with zeros. The pilots are used to estimate the channel between a transmitting antenna and a receiving antenna.

The blocks and the processes used on the Base Station transmitter are going to be introduced in the following pages.

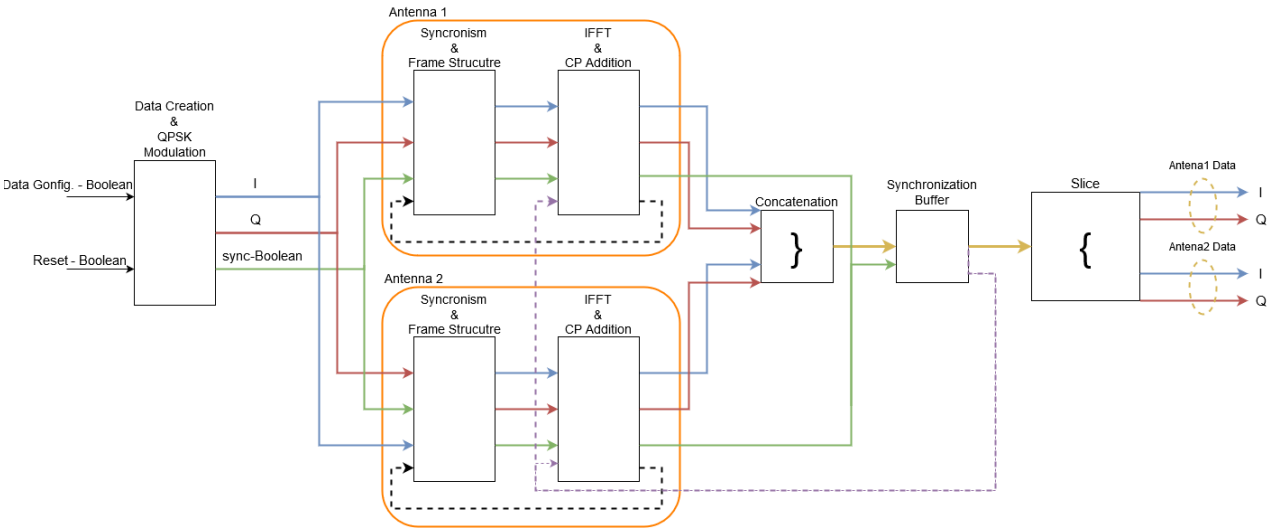

Figure 4.4: Base station transmitter block model.

The *Data Creation & QPSK Modulation* block, represented on figure 4.5, uses a Linear Feedback Shift Register (LFSR) to generate pseudo-random sequences of bits. The data is then modulated by a finite-state machine, that does the QPSK modulation to each pair of bits coming from the LFSR. At the output of the QPSK modulation block, we get the In-phase (I), real value, and Quadrature (Q), imaginary value, of the each QPSK symbol, along with a sync Boolean that is used to synchronize and count the number of symbols. The LFSR was configured so that every signal created by it starts with the word "F5555555". This was done with the objective of facilitating the synchronism blocks at the receivers. As every signal begins with the same sequence of bits it allows for easier recognition and synchronization at the receiving end.

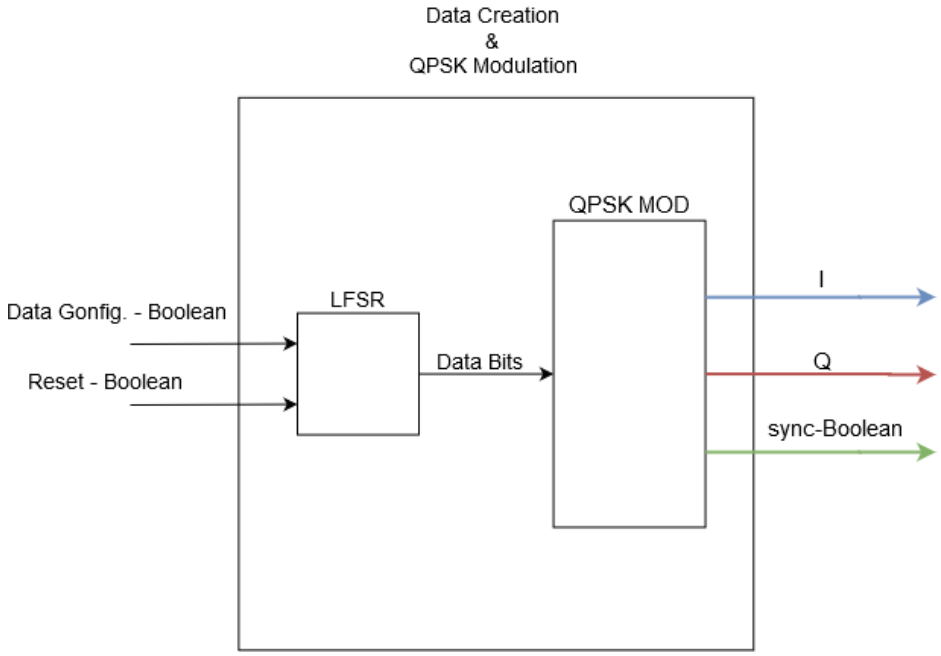

Figure 4.5: QPSK and Data Generation block model.

Subsequent to the creation of the data symbols, the *Synchronism & Frame Structure* block, depicted in figure 4.6, that organizes the data symbols and the pilots to their respective carriers that will then be modulated as an OFDM symbol. Additionally, this block also determines the transmission of OFDM symbols which is organized in frames that were defined prior to hardware implementation. The signal transmission frame consists of a synchronization OFDM symbol (Zadoff-Chu) and three symbols with data and pilot carriers. The information of this frame is stored in a vector variable called *subframe* and can be changed according to the users needs. The type of data that goes into each of the OFDM's carriers, is also codified in a ROM according to their index position in the frequency spectrum. This process starts with the Frame Coordination block that is implemented with several finite-state machines, that uses both the information of the *subframe* vector and the codified ROM to select the right output from the multiplexers. This output can be a zero a QPSK data symbol or a pilot symbol. The pilots are generated by the *Pilot Generator* using a LFSR and are QPSK modulated. In the receiver a similar pilots generator is built which synchronizes with the beginning of an OFDM symbol frame. This way the received reference signals are compared to the transmitted symbols and the channel response for those frequencies can be calculated.

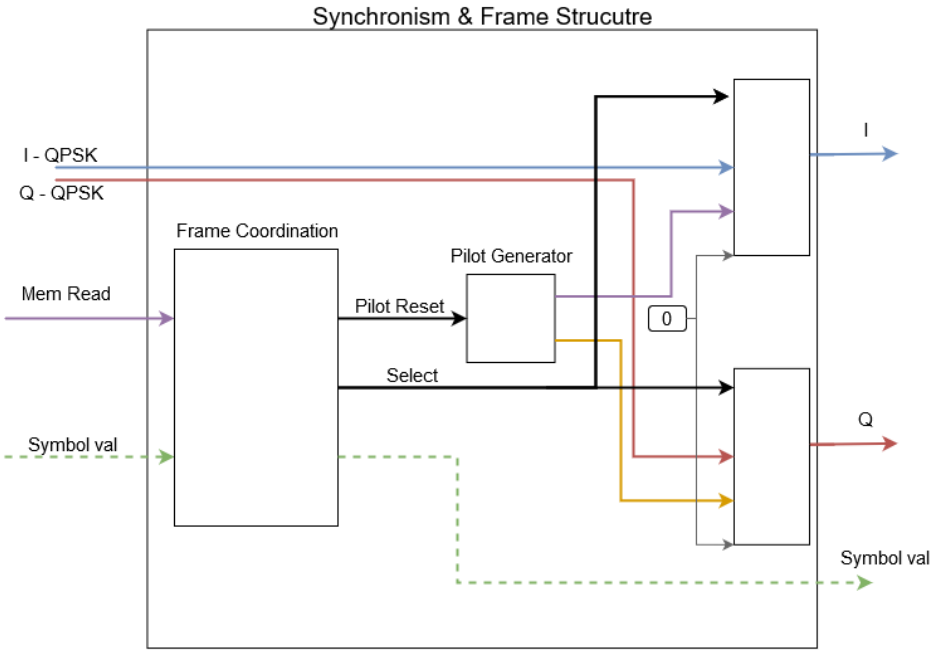

Figure 4.6: OFDM Symbol Framing block model.

Once the OFDM symbol is assembled it is processed by the*IFFT & CP Addition* block. The synchronization symbol is not processed by the IFFT but it is added at the beginning of the transmission frame in the time domain. For that a dummy symbol where all carriers are equal to zero is processed by the IFFT and, at the output of the IFFT, the index generated by its core is used to address a ROM in which is stored the time

domain Zadoff-Chu samples. An example of the output signals of this block obtained from a simulation can be seen in figure 4.8, where the first two graphs represent the I and Q values and the last is the Boolean *Symbol Val* that validates each OFDM or zadoff-chu symbol.

The OFDM symbol consists of 1024 carries in which 600 are used for data and pilots. The remaining carriers are left as band guards. The used OFDM symbol frame was designed to insert a pilot symbol for every two data symbols in a sequence of three carries. In this system , every OFDM symbol has both pilots and data symbols, although this frame structure can be changed. As our system uses two antennas, the frames for each antenna are different, as the pilot symbols are interpolated in order to grant channel estimation. Part of our OFDM symbol organization is represented in figure 4.7, where *A1* corresponds to the pilots transmitted by the first antenna, *A2* the pilots transmitted by the second antenna and *D* the data symbols (the numbers on the bottom correspond to the number of the respective carrier).

x	D	D	A1	D	D	x	D	D	A1
A2	D	D	x	D	D	A2	D	D	x
304	305	306	307	308	309	310	311	312	313

Figure 4.7: OFDM symbol frame example.

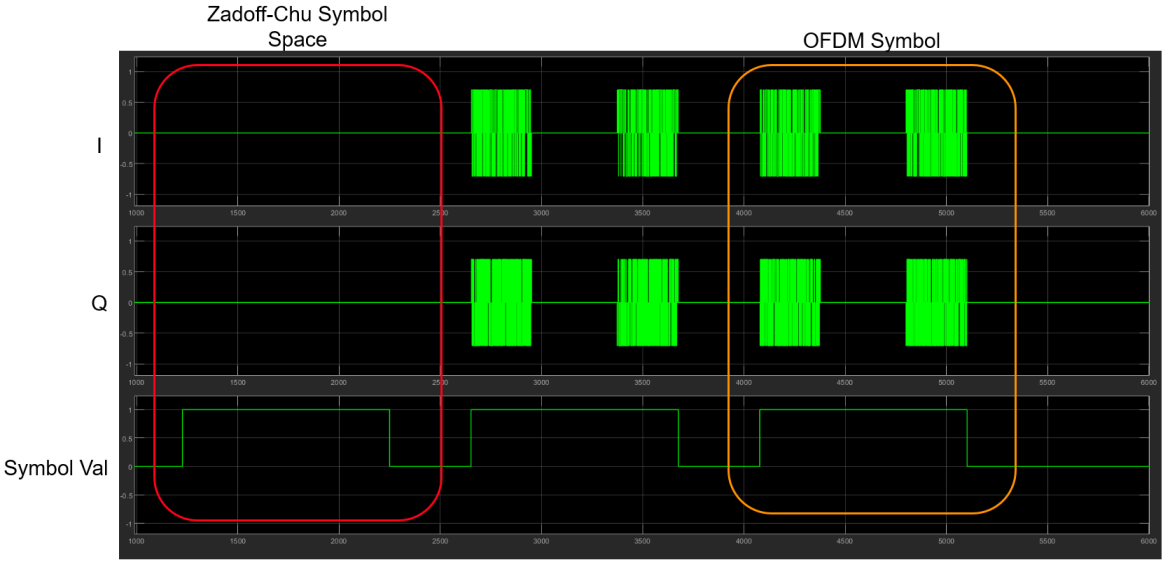

Figure 4.8: *Synchronism & Frame Structure* block outputs.

Following the OFDM symbol assembly, we proceed with the calculation of the IFFT of each carrier, and the addition of the CP to each OFDM symbol. These block are represented in figure 4.9. This process starts with the calculation of the IFFT of each carrier until the last one while counting their corresponding index. The output of the IFFT block corresponds to the in-phase and quadrature values of the symbol, the Boolean *ifft_ div* that keeps track of the symbol synchronism and the corresponding carrier index that is necessary for the following block.

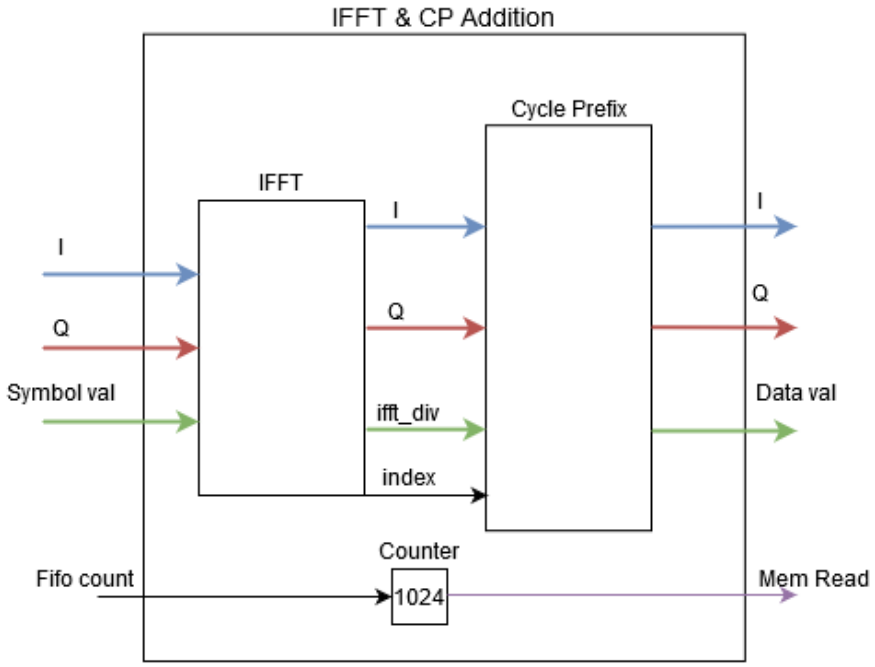

Figure 4.9: IFFT and Cycle Prefix block model.

Following the IFFT block comes the The *Cycle Prefix* block. In this block there is a core to add, when required, the synchronization(zadoff-chu) symbol pior to the CP addition. The *Cycle Prefix* block adds 256 samples of the OFDM symbol, post the IFFT calculation. Meanwhile, there is counter that keeps track of the number of carries processed and restarts every time the *Synchronization Buffer's* FIFO requires more symbols to achieve a continuous transmission.

Table 4.1: Implemented OFDM symbol structure.

Total carriers	1024
Data and pilot carriers	600
band guard carriers	424
CP samples	256

Lastly, both OFDM symbols from each antenna are concatenated into a single stream and stack into a FIFO in the Synchronization Buffer, as represented on figure 4.4. This buffer stacks enough symbols to create a continuous signal upon their transmission. These are then sliced and finally transmitted. This feature was added specifically to obtain a continuous signal.

4.2 User Terminals

All OFDM receivers require some form of frame detection and synchronization to guaranty that the number of samples extracted belong to an unique transmitted symbol. The receivers and also require a channel estimation method to be able to demodulate the received signal properly. Therefore, both UT1 and UT2 share the same receiving blocks. In figure 4.10 it is represented the block diagram of those common cores. It consists of a frame detection and synchronization (*Frame Detection & Synchronism* block), a OFDM demodulator and a core to perform channel estimation and interpolation(*FFT & Channel Gain Calculation* block). This receiver scheme was designed for a single antenna to recover the signal from a transmitter equipped with two antennas. Therefore, UT2 uses two of these schemes, one for each of its antennas, in order to implement the filter W_s to the incoming signals of the two antennas from the BS transmitter. This section will start with a basic explanation of the receiving scheme and its blocks, as they are common to both users. Then, an analysis of the equalization and the filter implementations will be done, separately, and with more detail as they were created particularly for this project. The received signals (I_in, Q_in) contain the OFDM symbols and the channels gains.

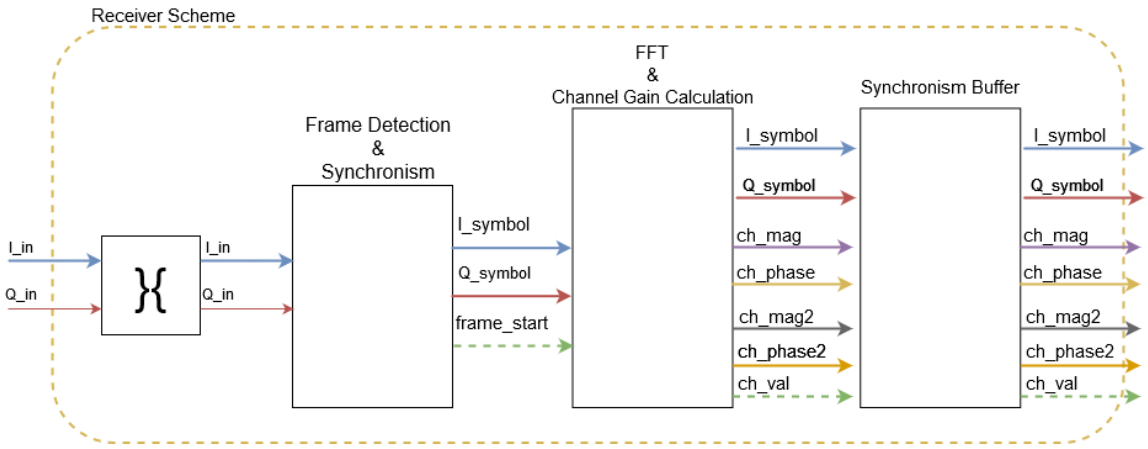

Figure 4.10: Receiver Scheme model.

The received signals pass through the frame detection block as depicted on figure 4.11. The frame start detection and synchronization is performed in two steps, first a matched filter detects the Zadoff-Chu symbol and secondly a correlation is made between the received OFDM symbol and a delayed version of himself. The delay is equal to the number of carries of the OFDM symbol, 1024. When comparing those two signals there is a peak in power when the CP overlaps in both signals. The matched filter produces a very high peak which opens a time window during which a finer search for frame start detection is conducted. The matched filter detection is done at a rate 16 times lower than the rest of the process. Once the beginning of the frame is detected the the first symbol is discarded since it corresponds to the synchronization symbol. Then, with the information of each *frame_start* the OFDM symbols go through the *CP Remover* block where the CP is removed. This block outputs the in-phase and quadrature data, along with the frame start (*I_data, Q_data, frame_start*).

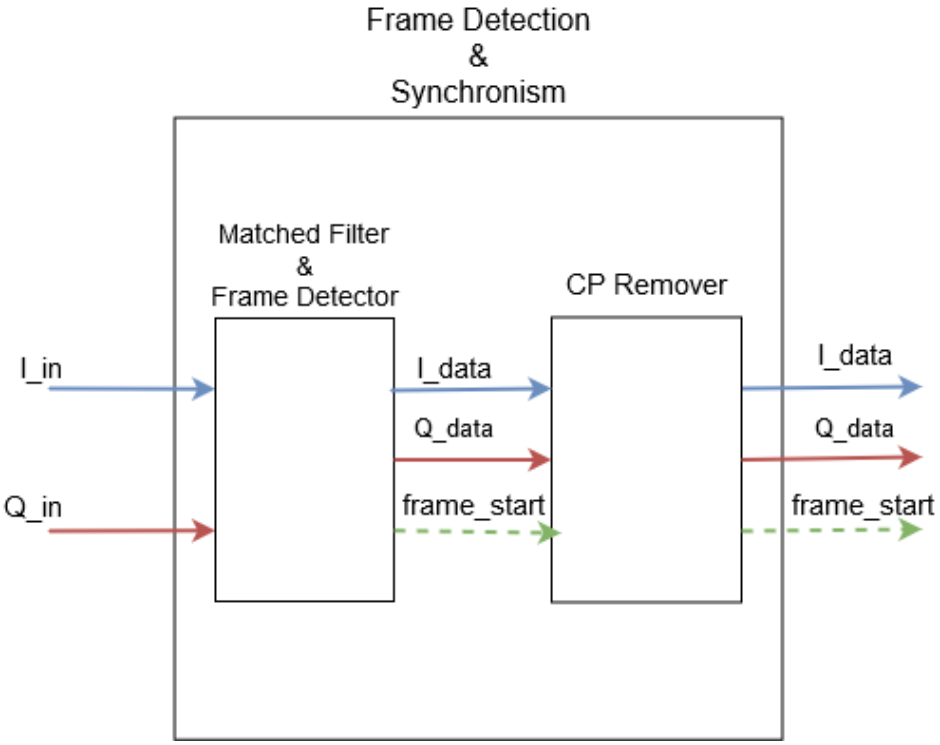

Figure 4.11: Frame Detection block model.

After the frame detection block, follows the *FFT & Channel Gain Calculation* block. In this part of the receiver, the OFDM symbols are recovered and all their carriers indexed and synchronized with respective the data signals. Additionally, the channel's gains are estimated with the pilots from the two transmitting antennas. This process begins with a buffer that does the indexing and synchronization of the input data signals (*I_ data Q_ data*) by resourcing the frame start information given by the previous block. Then, the input signals pass through an FFT block and are converted into their polar representation using the magnitude and phase of each symbol. This last step is done in order to estimate the two different channels as they pass through the blocks *Channel Estimator* 1 and 2. Both Channel estimating blocks are synchronized by the *val* and *frame_ start* signals, and execute the same process for channel estimation. The only difference between blocks is the pilots used to determine each channel gain. They begin with the removal of the pilots from the OFDM symbol using their corresponding pilot frame map. Then, they apply a linear interpolation to determine both the magnitude and the phase of the channel gains. At the end, we obtain the data signals post-FFT which are synchronized by *div_ Data*, and the two channel gains from each transmitting antenna in their polar presentation synchronized by *ch_ val*.

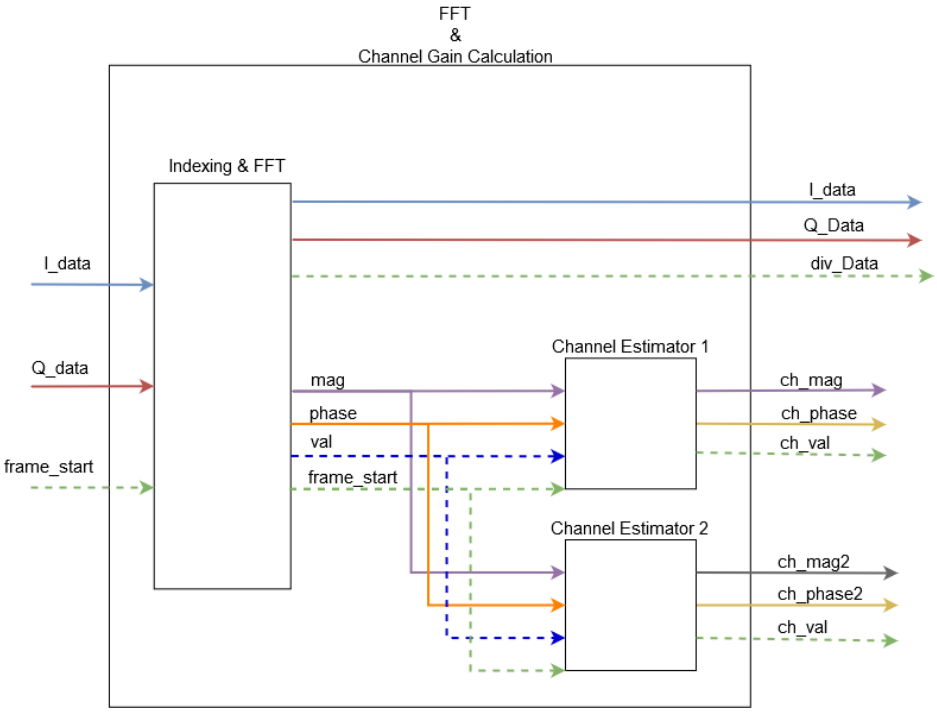

Figure 4.12: FFT block model.

The receiving process ends with the organization of the channel gains with its corresponding data symbol, as all the outputs from the FFT block go through a buffer that synchronizes all the signals and creates a single Boolean (ch_val) that establishes the rate of the signals. Finally, all the information required to apply the specific demodulation algorithms is ready.

4.2.1 UT1 Equalization

As presented in section 3.2.2 the UT1 equalization requires complex multiplications and addition. Unlike high level programming, the manipulation of complex numbers is not straightforward when implemented in hardware. Therefore, the explanation of the used process is divided in three different sections, each one with its propose. The blocks used on system generator are depicted on figure 4.13.

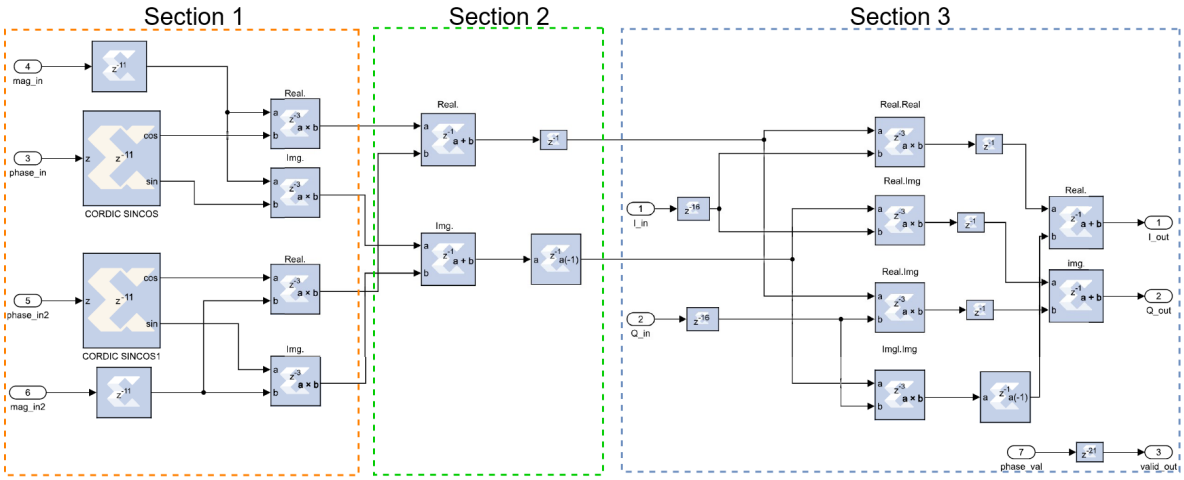

Figure 4.13: Implemented main user equalizer.

Section 1

This section does the conversion of the channel's elements (*mag_in, phase_in, phase_in2, mag_in2*) from their polar representation to cartesian, to keep a common structure between the channel's gains and the received signal, and also to be possible to apply the equalization. This conversion is done by determining the cos and the sin values of the channel phase and then multiplying in by its corresponding magnitude. For this operation, a CORDIC block was used to calculate the phase values, a delay block to keep synchronization between the magnitude and the phase signal and, lastly, a multiplication block.

Section 2

Section two implements the equation (3.22), by adding each in-phase and quadrature values calculated in the previous section. Then, it finishes with the Hermitian operation by changing the signal value of the imaginary part. This operation uses only a sum block, a delay, and a not block.

Section 3

The last section completes the operation described at equation (3.23) by applying the distributive property to the symbol with the channel gain, previously referred to as $\mathbf{x_{p,G}}$. The received signal is also represented in the cartesian form, with its respective in-phase and quadrature values (*I_in, Q_in*). Each multiplication block performs its respective function followed by the sum of the real and imaginary products. This section was designed with a delay block to keep the received signal synchronized with the rest of the operation, multiplication blocks, a not block to change the signal of the multiplication between both imaginary components and the sum blocks.

The overall design and implementation of this equalization can be done with different blocks and by applying different manipulations. This design was done with the objective of a future hardware implementation that would not suffer from time constraints upon implementation, as this problem is usually related to more complex manipulations as signal multiplexing. Therefore, this process was divided into multiple, but simple, operations.

After the equalization, the signals are sent to a QPSK demodulation block that converts the QPSK symbols into the original bit words created at the transmitter's LFSR. Subsequently, the bits go to a block that compares the received bits with the one created at the transmitter for the BER determination.This way the bit error rate can be estimated in real time

4.2.2 UT2 Receiver

This section will end with the description of the static method filter created for this project. As stated earlier the UT2 uses two of the receiving schemes presented on section 4.2 since this user is equipped with two antennas. Therefore, there is double the number of channel gains to process, compared to the UT1. The scheme implemented is represented on figure 4.14, where the depicted inputs are the data symbols from each antenna and the channel gains. This scheme can be divided into two main sections. The first section consists of the $\mathbf{F_s}$ matrix inversion and $\mathbf{W_s}$ creation. The second section is the filter application on the data symbols.

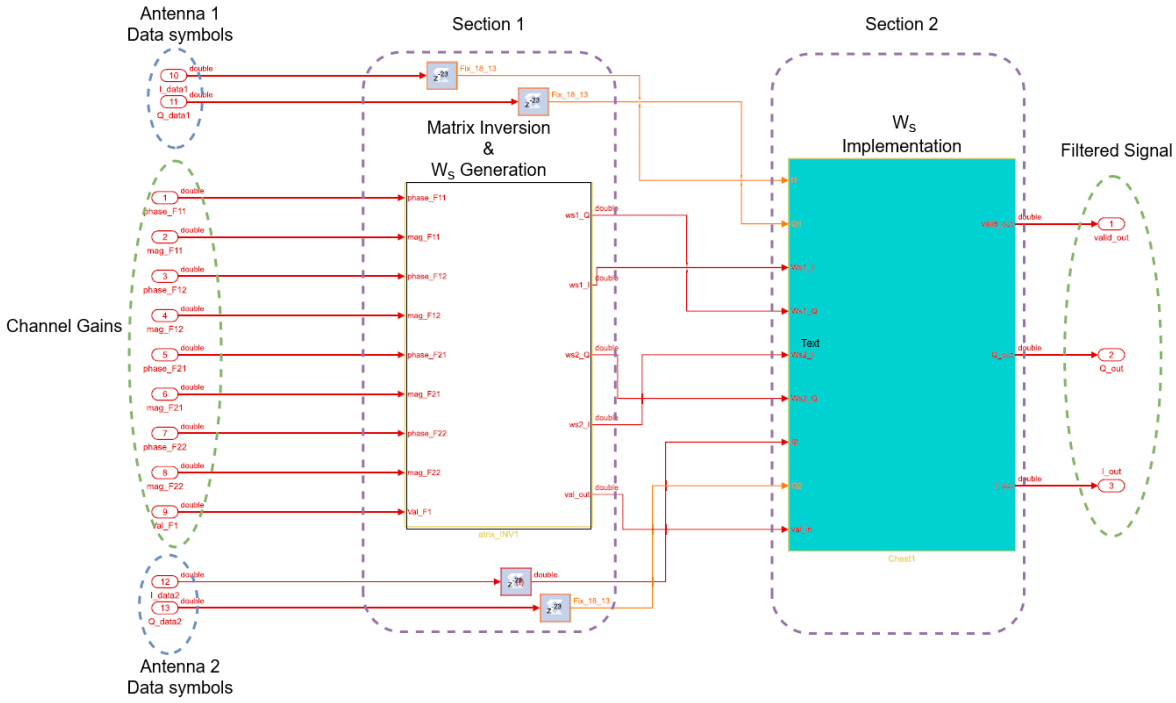

Figure 4.14: Second User implemented filter.

Section 1

The matrix inversion and filter generation, which block are depicted in figure 4.15, start with the conversion of the channel gains from their polar form to their cartesian values. This operation was done by using the same method and blocks as in section 4.2.1.

Subsequently, the $\mathbf{F_s}$ matrix inversion begins by following the properties written in equation (3.27). The inversion starts with the calculation of the determinant by the *Determinant Calculation* block as represented on figure 4.15. This process was done by applying the same method as implemented in section 4.2.1 to perform the multiplication between channel gains. Then, the inverted value of the determinant is calculated so that its division as in equation (3.27) may occur. This step is done in the *Determinant Inversion* block depicted in figure 4.15.

The W_s *Generation* block is where the reorganization and the division happen completing the $\mathbf{W_s}$ matrix creation. This block receives as in-puts the cartesian values of the $\mathbf{F_s}$ matrix as well as the inverted value of its determinant. The channel gains are reorganized into the inverse matrix and finally summed according to equation (3.28), resulting into the W_s filter vector equation (3.29) that is the final output of the Matrix Inversion and W_s *Generation* block at figure 4.14.

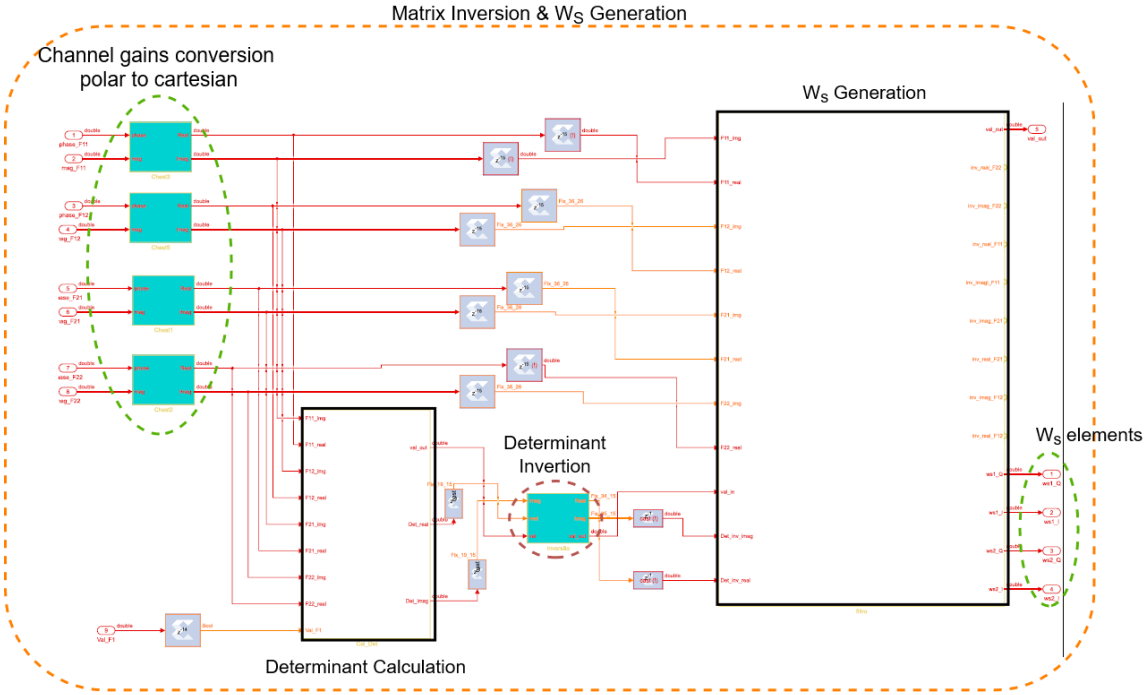

Figure 4.15: Matrix Inversion and Filter generator implemented blocks.

Section 2

Subsequently, the W_s *Generation* block outputs go to the W_s Implementation block, along with the data signals (I_1, Q_1, I_2, Q_2) provided by the OFDM receiving blocks. The W_s Implementation block is where the equation (3.30) operation is performed. The blocks used for this process are represented in figure 4.16. The method used for the multiplication and sum between the W_s elements and the data symbols is identical to the one used on section 4.2.1 of the UT1. Then the post filtered signals are "cleaned" of any imperfections from the mathematical manipulations by going through two FIFOs, one for the in-phase value and the other of the quadrature value. The UT2 ends at the filter and since the signals are to be cancelled there is no demodulation nor BER calculations. Similar to the UT1, this scheme was designed to avoid multiplexing systems as these can result in time constraints in upon hardware implementation.

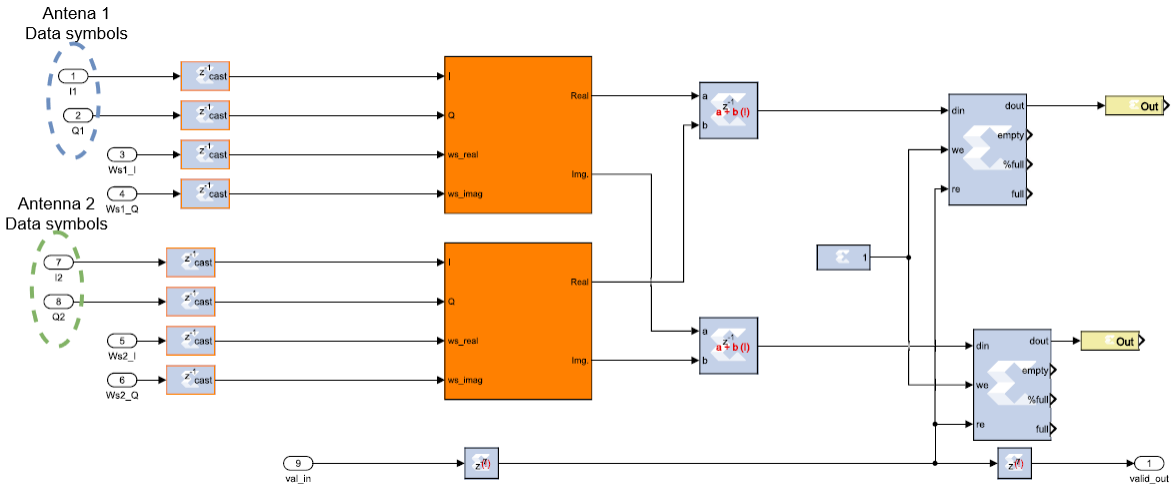

Figure 4.16: W_s Implementation block.

In the next section, we will analyze and present the tests done to the previous schemes followed by the respective results obtained.

4.3 Tests and Results

This section will introduce the tests done to the implemented systems in system generator and their correspondent results. The tests were done with the objective of not only testing the main objectives set to each UT, but also their overall functioning in terms of synchronization, channel estimation, and hardware resource use. In addition to the functionality test, the main user's SNR response was measured. Both the procedures and measurements will be presented on the following pages.

4.3.1 UT1 tests

The UT1 was tested in two different ways. The first test was done with no noise addition and with a fixed channel. The channel was simulated by adding again to the signal prior to its transmission. The system implemented is represented on figure 4.17, where the outputs of the transmitter are summed to simulate the single stream that would be received at the UT1. The simulation ran over 715 OFDM symbols, which in our system represents 286K QPSK data symbols, that total 572K transmitted bits. This test was done with the objective of measuring the overall performance of both the transmitter and receiver scheme in a perfect environment. The most important measurements from this test were the channel estimation done by the reception, the correct demodulation of the received signals, the BER rate, and the resource usage estimation for hardware implementation. Although the system generator simulation has its own BER calculation block, the received signal at the UT1 was also loaded to Mathlab in order to further analyze the results.

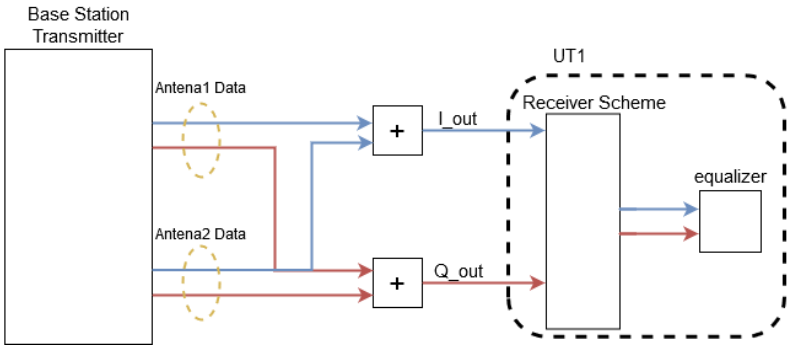

Figure 4.17: UT1 test model.

Results UT1

Subsequently to the pilots removal, the receiving system determines both the phase and the amplitude of the channel in each OFDM symbol. As it was expected the receiver successfully estimates the channel gains. The phase and amplitude of one of the channel G elements are

represented on figure 4.18, respectively. The figure represents the channel gains estimated with one of the OFDM symbols. As the channel is fix and there is no noise, the phase is mostly linear, and the channel's amplitude is static.

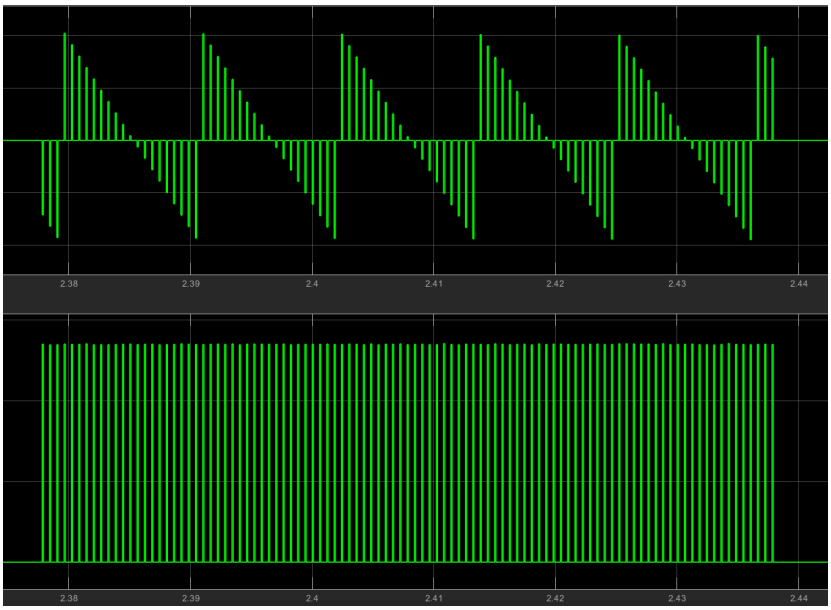

Figure 4.18: Channel phase and amplitude estimation.

The system generator model processed all the 286K QPSK symbols with no errors, as expected. The simulated signals were then processed on Mathlab to acquire the constellations on figure 4.19, which represents the successfully transmitted signals before and after their demodulation. Analyzing the constellation pos-equalization, one can conclude that the system is working properly as all the symbols are clearly in one of the four quadrants.

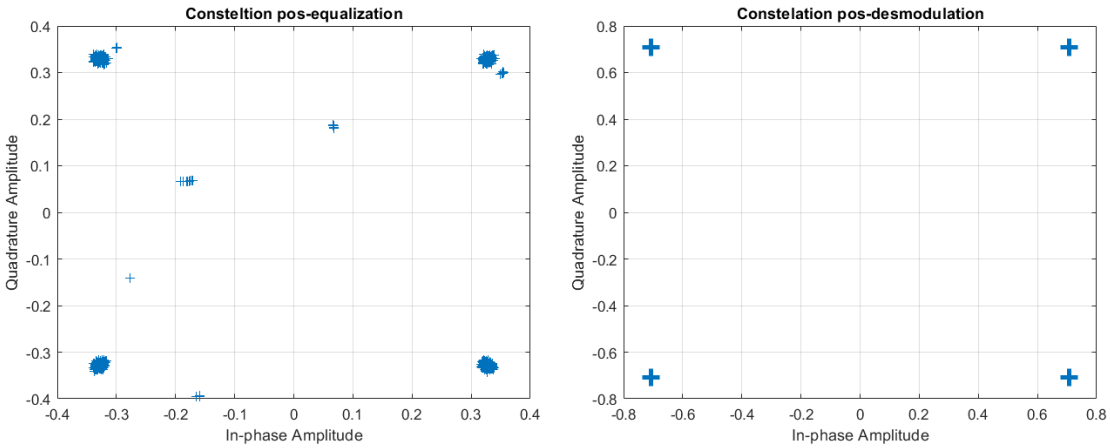

Figure 4.19: QPSK symbol constellations.

Using the tools provided by Xilinx, an estimation of the total hardware resources needed to

implement this model was done on both the transmitting and receiving sides of the model. The following tables XY show the resources used by the transmitter and the receiver, respectively. In the tables is represented the total number of Look-up-tables, Look-Up Table as Distributed Ram (LUTRAM), Flip Flops (FF), Block Rams (BRAM), Digital Signal Processors (DSP) and Input-Output blocks (IO).

Table 4.2: Main User System Requirements.

Resource	Transmitter	Receiver
LUT	9542	18040
LUTRAM	3174	4075
FF	14192	22752
BRAM	53.50	236
DSP	24	89
IO	4	3

UT1 SNR test

The second test performed to the UT1 had the goal of measuring its BER performance for different SNR levels. To accomplish this, a system like the one represented on figure 4.20, was implemented. A noise block was added between the transmission. Then, several simulations were done for different values of noise power calculated according to different values of SNR, that varied from 0 to 20dBs. Unlike the first test, only 143K QPSK symbols were simulated for each noise power level. The obtained values from the simulation were then compared theoretical equivalent process done in Matlab, with the objective of verifying the robustness of the implemented system figure 4.21.

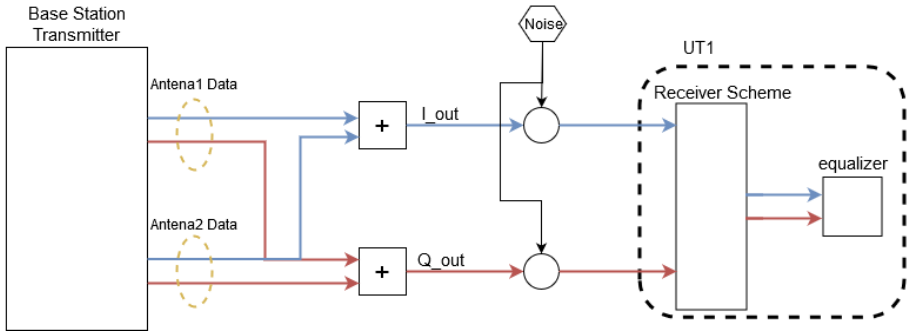

Figure 4.20: UT1 SNR test model.

4.3.2 UT2 test

The second user was tested only once, with a system similar to the one represented on figure 4.22. Has this user must cancel the incoming signals, no demodulation system nor BER

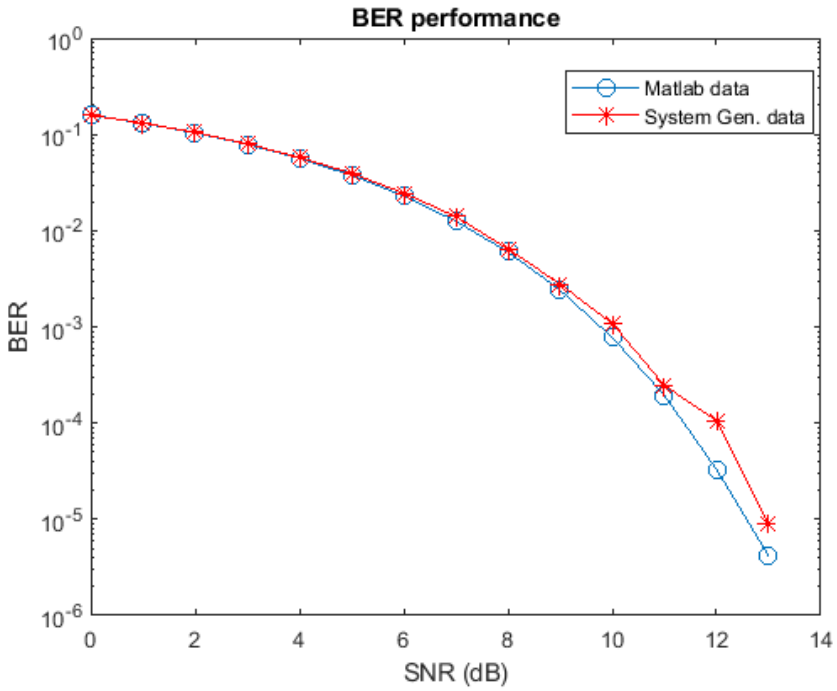

Figure 4.21: UT1 SNR test results.

calculation blocks were implemented. Thus, the test was totally done on the system generator model. To simulate the different channels of each receiving antenna, the incoming signals pass through a block that adds a delay and attenuates both signals, before they are injected to both receiving schemes of the UT2. For better visualization of the cancellation of the signals,

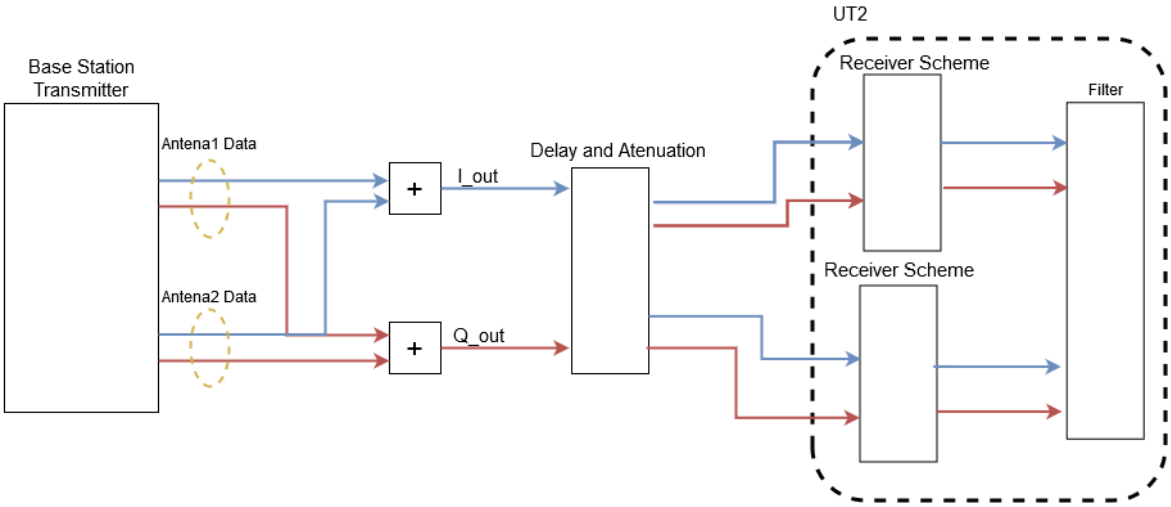

Figure 4.22: UT2 test model.

let us consider the last block implemented to the UT2 receiver, depicted on figure 4.23, where

the filter matrix W_s is applied to the signals from both antennas. As represented on the figure 4.23 there are three different points worth checking that show the different steps taken for the cancellation of the received signal. At the first point, we can see the "raw" in-phase value of the incoming OFDM symbols, that were only used for channel estimation. The second point the signal is post-filtering, at this point the incoming signal is canceled almost entirely. Both signals are represented on figure 4.24. In this figure we can see three different graphics, the first one represents the Boolean variable val_in that represents the beginning and the end of the OFDM symbol, while the second and the third graphics the difference between the received and the filtered signals. At the third and last point, the signal is cleaned and only the rest of the OFDM symbol remains. The difference between signals can be seen on figure 4.25, which the first graphic we have three pulses of the val_in variable, where each pulse represents a symbol, as well as a zoomed-in representation both signals in point two and three. Lastly, a recourse estimation was also done to the receiving block, as represented intable 4.3.

Table 4.3: Second User System Requirements.

Resource	UT2 Receiver
LUT	10437
LUTRAM	4817
FF	13350
BRAM	9
DSP	46
IO	4

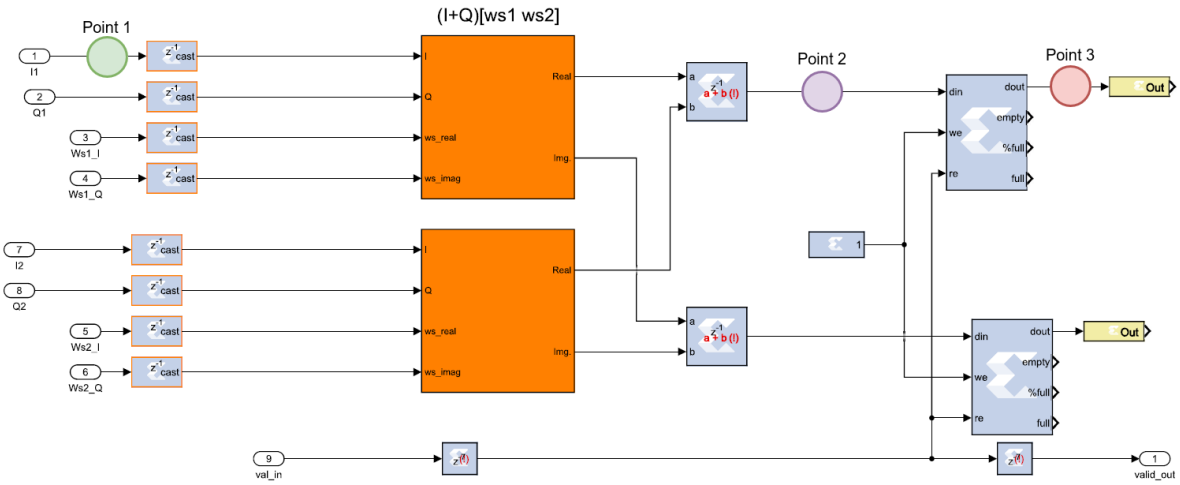

Figure 4.23: Filter block.

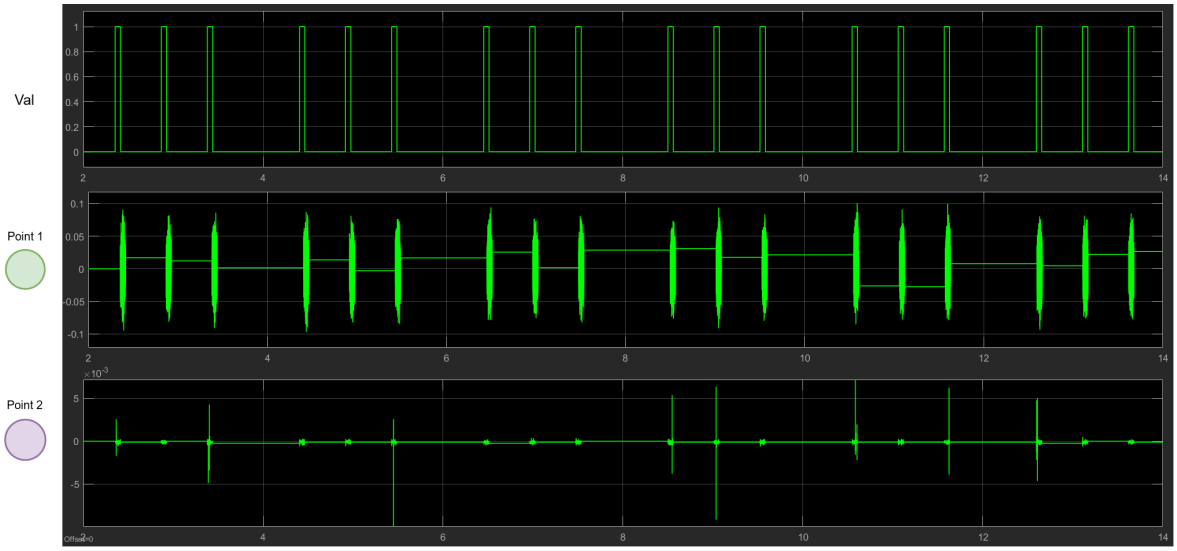

Figure 4.24: UT2 cancellation results.

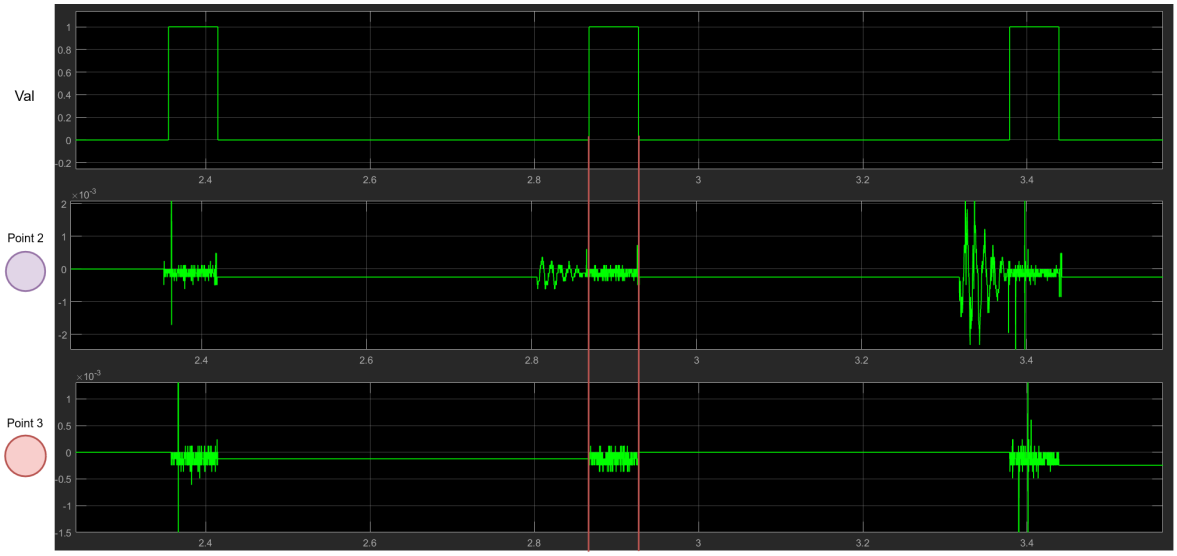

Figure 4.25: UT2 cancellation results.

Chapter 5

Tests, Results and Conclusions

In this chapter it will be drawn the conclusions from the obtained results as well as the proposal and considerations for future work.

5.1 Conclusion

The work presented in this dissertation is a follow up of the conjunction of efforts to create an efficient interference mitigation technique based on IA, that would allow the coexistence between the small-cells (secondary users) and the macro-cell (primary users) in a HetNet. This master thesis focused specifically on giving the first step on the hardware implementation and evaluation of an interference mitigation technique. This algorithm had been previously proposed and tested, but never brought into a real-time platform before citesyed [27]. The objective of this technique is to cancel the downlink interference from a base station to the secondary users within its coverage, while still allowing for an effective connection to the primary users. The technique implemented was the Static Method, which requires no channel information shared between the different terminals of the network. The end goal was to create IP using the hardware modeling toll System Generator, hence, conceiving the foundation for future hardware implementation. Therefore, by analyzing the results previously displayed we will draw a conclusion and inquire if the objective were meet.

UT1 Implementation

The UT1 was design with the objective of successfully receiving the transmitted signals by the BS, hence two tests were performed in order to study the design's performance and state for future hardware testing. The first test was done with the intent of proofing that the design has no flaws when used on a perfect environment, thus the transmission and reception of the data signals was done through a perfect channel with no additive noise. When examining results on section 4.3.1 it is safe to conclude that the designing system functions properly in

a perfect environment meeting the theoretical expectations of such test. The second test was done in order to evaluate the UT1 design performance for different levels of SNR as well, as compare its behavior to the theorize results obtained in a similar simulation run on Matlab. This test results displayed on section 4.3.1, prove that the design is ready to be tested on hardware as its results are virtually identical to the ones obtained by Matlab.

UT2 Implementation

The UT2 had as main directive to successfully cancel the incoming signals from the BS, therefore a single test was performed in order to test the static method cancellation effectiveness. The results presented on section 4.3.2 one can conclude that the created design is also ready to be implemented in hardware, as the incoming signals from the BS are virtually canceled when compared to the received signal prior to the filter block.

In resume, with the work accomplished by this thesis, there were created two IP fully functional and ready to be tested on a FPGA, to continue the this projects scope of implementing an interfering mitigation method for HetNets based on IA.

5.2 Future Work

Although the two designs were successfully generated there is still room for improvements in different aspects. Therefore this thesis will finish with some suggestions for the future work. The improvements can be made in the following points:

- **Hardware Implementation**: Due to the time in which this master thesis was done, there were severe constrains on hardware testing and development of the designed blocks. Thus, the logical follow up to the work done is the cross over of the created IPs on System Generator, to a more suited hardware designing and programming tool such as Vivado, to verify the schemes true functionality.

- **Synchronization and Speed**: The designs should be reassessed in terms of speed and synchronization. Although functional, the design of the transmitter might face some problems due to the number of buffers and also its necessity to read and store information of the transmitting signals in RAM slots. With the development of the design for the secondary user, it was noticed that the cancellation of the incoming signals became significantly more efficient, upon a synchronization upgrade done to the Frame Detection and channel estimation blocks. Hence, working towards a more robust system in terms of signal synchronization will improve the designs performance.

- **More efficient hardware resource use**: As stated before both receivers designs were done without any signal multiplexing due to possible time constrains that the designs might suffer upon hardware implementation, that will require more attention to the

system's signal synchronization. However, by multiplexing the incoming signal into a single stream of information, can reduce the number of blocks used by half ultimately reducing the resources needed for its hardware use.

References

[1] A. Gawas, "An overview on evolution of mobile wireless communication networks: 1g-6g," *International Journal on Recent and Innovation Trends in Computing and Communication*, vol. 3, no. 5, pp. 3130–3133, 2015.

[2] H. Mehta, D. Patel, B. Joshi, and H. Modi, "0g to 5g mobile technology: A survey," *J. of Basic and Applied Engineering Research*, vol. 1, no. 6, pp. 56–60, 2014.

[3] M. R. Bhalla and A. V. Bhalla, "Generations of mobile wireless technology: A survey," *International Journal of Computer Applications*, vol. 5, no. 4, pp. 26–32, Aug. 10, 2010, ISSN: 09758887. DOI: 10.5120/905-1282.

[4] A. Kukushkin, *Introduction to Mobile Network Engineering: GSM, 3G-WCDMA, LTE and the Road to 5G*. John Wiley & Sons, 2018.

[5] M. A. Hitt, B. W. Keats, and S. M. DeMarie, *Navigating in the new competitive landscape: Building strategic flexibility and competitive advantage in the 21st century*, 4. Academy of Management Briarcliff Manor, NY 10510, 1998, vol. 12, pp. 22–42.

[6] S. Patel, V. Shah, and M. Kansara, "Comparative study of 2g, 3g and 4g," *nternational Journal of Scientific Research in Computer Science, Engineering and Information Technology*, vol. 3, pp. 2456–3307, 3 Sep. 20, 2018.

[7] L. Yuan, "Research on OFDM technology in 4g," in *Information Computing and Applications*, Y. Yang, M. Ma, and B. Liu, Eds., ser. Communications in Computer and Information Science, Berlin, Heidelberg: Springer, 2013, pp. 11–19, ISBN: 978-3-642-53703-5. DOI: 10.1007/978-3-642-53703-5_2.

[8] C. Cox, *An introduction to LTE: LTE, LTE-advanced, SAE and 4G mobile communications*. John Wiley & Sons, 2012.

[9] S. Parkvall, E. Dahlman, A. Furuskar, Y. Jading, M. Olsson, *et al.*, "Lte-advanced-evolving lte towards imt-advanced," in *2008 IEEE 68th Vehicular Technology Conference*, IEEE, 2008, pp. 1–5.

[10] J. O'Halloran. (Feb. 27, 2020). "5g now available in 378 cities globally." C. Weekly, Ed., [Online]. Available: https://www.computerweekly.com/news/252479242/5G-now-available-in-378-cities-globally.

[11] F. Boccardi, R. W. Heath, A. Lozano, T. L. Marzetta, and P. Popovski, "Five disruptive technology directions for 5g," *IEEE Communications Magazine*, vol. 52, no. 2, pp. 74–80, 2014.

[12] J. G. Andrews, S. Buzzi, W. Choi, S. V. Hanly, A. Lozano, *et al.*, "What will 5g be?" *IEEE Journal on Selected Areas in Communications*, vol. 32, no. 6, pp. 1065–1082, 2014.

[13] I. Parvez, A. Rahmati, I. Guvenc, A. I. Sarwat, and H. Dai, "A survey on low latency towards 5g: Ran, core network and caching solutions," *IEEE Communications Surveys Tutorials*, vol. 20, no. 4, pp. 3098–3130, 2018.

[14] S. Ullah, K.-I. Kim, K. H. Kim, M. Imran, P. Khan, *et al.*, "Uav-enabled healthcare architecture: Issues and challenges," in *Future Generation Computer Systems*, 2019.

[15] H. Ullah, N. Gopalakrishnan Nair, A. Moore, C. Nugent, P. Muschamp, *et al.*, "5g communication: An overview of vehicle-to-everything, drones, and healthcare use-cases," *IEEE Access*, vol. 7, pp. 37 251–37 268, 2019.

[16] "5g use cases and requirements white paper," Nokia, Finlad, 2016. [Online]. Available: `https://www.ramonmillan.com/documentos/bibliografia/5GUseCases_Nokia.pdf`.

[17] "Cisco annual internet report (2018–2023) white paper," Cisco, Mar. 9, 2020. [Online]. Available: `https://www.cisco.com/c/en/us/solutions/collateral/executive-perspectives/annual-internet-report/white-paper-c11-741490.pdf`.

[18] M. Agiwal, A. Roy, and N. Saxena, "Next generation 5g wireless networks: A comprehensive survey," *IEEE Communications Surveys Tutorials*, vol. 18, no. 3, pp. 1617–1655, 2016.

[19] T. S. Rappaport, S. Sun, R. Mayzus, H. Zhao, Y. Azar, *et al.*, "Millimeter wave mobile communications for 5g cellular: It will work!" *IEEE Access*, vol. 1, pp. 335–349, 2013.

[20] M. Agiwal, A. Roy, and N. Saxena, "Next generation 5g wireless networks: A comprehensive survey," *IEEE Communications Surveys Tutorials*, vol. 18, no. 3, pp. 1617–1655, 2016.

[21] L. Lu, G. Y. Li, A. L. Swindlehurst, A. Ashikhmin, and R. Zhang, "An overview of massive mimo: Benefits and challenges," *IEEE Journal of Selected Topics in Signal Processing*, vol. 8, no. 5, pp. 742–758, 2014.

[22] D. Muirhead, M. A. Imran, and K. Arshad, "A survey of the challenges, opportunities and use of multiple antennas in current and future 5g small cell base stations," *IEEE Access*, vol. 4, pp. 2952–2964, 2016.

[23] T. Wang, P. Li, X. Wang, Y. Wang, T. Guo, *et al.*, "A comprehensive survey on mobile data offloading in heterogeneous network," *Wireless Networks*, vol. 25, no. 2, pp. 573–584, 2019.

[24] A. Damnjanovic, J. Montojo, Y. Wei, T. Ji, T. Luo, *et al.*, "A survey on 3gpp heterogeneous networks," *IEEE Wireless Communications*, 2011.

[25] W. Stallings, *Data and computer communications*. Pearson/Prentice Hall, 2007.

[26] S. S. Ali, "Physical-layer cooperative interference mitigation techniques for wireless heterogeneous systems," Aveiro University Department of Electronics, Telecommunications and Informatics, 2018.

[27] S. S. Ali, D. Castanheira, A. Silva, and A. Gameiro, "Downlink cognitive interference alignment for heterogeneous networks," in *2014 21st International Conference on Telecommunications (ICT)*, 2014, pp. 236–240.

[28] S. B. Weinstein, "The history of orthogonal frequency-division multiplexing [history of communications]," *IEEE Communications Magazine*, Nov. 2009.

[29] M. Viswanathan, "Simulation of digital communication systems using matlab," *Smashwords*, 2013.

[30] R. v. Nee and R. Prasad, *OFDM for Wireless Multimedia Communications*, 1st. USA: Artech House, Inc., 2000, 280 pp., ISBN: 978-0-89006-530-3.

[31] "Orthogonal frequency division multiplexing (ofdm) based uplink multiple access method over awgn and fading channels," Apr. 2019.

[32] H. Holma and A. Toskala, *LTE for UMTS: OFDMA and SC-FDMA based radio access*. John Wiley & Sons, 2009.

[33] M. Rumney, *Air Interface Concepts*. Wiley Online Library, 2013, pp. 11–89.

[34] S. Sanayei and A. Nosratinia, "Antenna selection in MIMO systems," *IEEE Communications Magazine*, vol. 42, no. 10, pp. 68–73, Oct. 2004, ISSN: 1558-1896. DOI: 10.1109/MCOM.2004.1341263.

[35] L. Zheng and D. Tse, "Diversity and multiplexing: A fundamental tradeoff in multiple-antenna channels," *IEEE Transactions on Information Theory*, vol. 49, no. 5, pp. 1073–1096, May 2003, ISSN: 1557-9654. DOI: 10.1109/TIT.2003.810646.

[36] M. Jankiraman, *Space-time codes and MIMO systems*. Artech House, 2004.

[37] S. Sesia, I. Toufik, and M. Baker, *LTE - The UMTS Long Term Evolution: From Theory to Practice*. John Wiley & Sons, Aug. 29, 2011, 817 pp., ISBN: 978-0-470-66025-6.

[38] J. G. Andrews, A. Ghosh, and R. Muhamed, *Fundamentals of WiMAX: understanding broadband wireless networking*. Pearson Education, 2007.

[39] E. G. Larsson, O. Edfors, F. Tufvesson, and T. L. Marzetta, "Massive MIMO for next generation wireless systems," *IEEE Communications Magazine*, vol. 52, no. 2, pp. 186–195, Feb. 2014, ISSN: 1558-1896. DOI: 10.1109/MCOM.2014.6736761.

[40] B. Das, M. P. Sarma, and K. K. Sarma, "Different aspects of interleaving techniques in wireless communication," in *Intelligent Applications for Heterogeneous System Modeling and Design*, IGI Global, 2015, pp. 335–374.

[41] V. Weerackody, "Method and apparatus for providing time diversity," U.S. Patent 5305353A, Apr. 19, 1994.

[42] D. Tse and P. Viswanath, *Fundamentals of wireless communication*. Cambridge university press, 2005.

[43] D. Astely, E. Dahlman, A. Furuskär, Y. Jading, M. Lindström, *et al.*, "LTE: The evolution of mobile broadband," *IEEE Communications Magazine*, vol. 47, no. 4, pp. 44–51, Apr. 2009, ISSN: 1558-1896. DOI: 10.1109/MCOM.2009.4907406.

[44] Y. Xin, Z. Wang, and G. Giannakis, "Space-time diversity systems based on linear constellation precoding," *IEEE Transactions on Wireless Communications*, vol. 2, no. 2, pp. 294–309, Mar. 2003, ISSN: 1558-2248. DOI: 10.1109/TWC.2003.808970.

[45] P. Mitran, H. Ochiai, and V. Tarokh, "Space-time diversity enhancements using collaborative communications," *IEEE Transactions on Information Theory*, vol. 51, no. 6, pp. 2041–2057, Jun. 2005, ISSN: 1557-9654. DOI: 10.1109/TIT.2005.847731.

[46] V. Tarokh, H. Jafarkhani, and A. Calderbank, "Space-time block codes from orthogonal designs," *IEEE Transactions on Information Theory*, vol. 45, no. 5, pp. 1456–1467, Jul. 1999, ISSN: 1557-9654. DOI: 10.1109/18.771146.

[47] V. H. M. Donald, "Advanced mobile phone service: The cellular concept," *The Bell System Technical Journal*, vol. 58, no. 1, pp. 15–41, Jan. 1979, ISSN: 0005-8580. DOI: 10.1002/j.1538-7305.1979.tb02209.x.

[48] J. G. Andrews, S. Buzzi, W. Choi, S. V. Hanly, A. Lozano, *et al.*, "What will 5g be?" *IEEE Journal on Selected Areas in Communications*, vol. 32, no. 6, pp. 1065–1082, Jun. 2014, ISSN: 1558-0008. DOI: 10.1109/JSAC.2014.2328098.

[49] T. Nakamura, S. Nagata, A. Benjebbour, Y. Kishiyama, T. Hai, *et al.*, "Trends in small cell enhancements in LTE advanced," *IEEE Communications Magazine*, vol. 51, no. 2, pp. 98–105, Feb. 2013, ISSN: 1558-1896. DOI: 10.1109/MCOM.2013.6461192.

[50] N. Saquib, E. Hossain, and D. I. Kim, "Fractional frequency reuse for interference management in LTE-advanced hetnets," *IEEE Wireless Communications*, vol. 20, no. 2, pp. 113–122, Apr. 2013, ISSN: 1558-0687. DOI: 10.1109/MWC.2013.6507402.

[51] K. I. Pedersen, Y. Wang, S. Strzyz, and F. Frederiksen, "Enhanced inter-cell interference coordination in co-channel multi-layer LTE-advanced networks," *IEEE Wireless Communications*, vol. 20, no. 3, pp. 120–127, Jun. 2013, ISSN: 1558-0687. DOI: 10.1109/MWC.2013.6549291.

[52] H. Claussen, L. T. Ho, and L. G. Samuel, "Financial analysis of a pico-cellular home network deployment," in *2007 IEEE International Conference on Communications*, IEEE, 2007, pp. 5604–5609.

[53] A. Khandekar, N. Bhushan, J. Tingfang, and V. Vanghi, "LTE-advanced: Heterogeneous networks," in *2010 European Wireless Conference (EW)*, Apr. 2010, pp. 978–982. DOI: 10.1109/EW.2010.5483516.

[54] Y. Zhou, L. Liu, H. Du, L. Tian, X. Wang, *et al.*, "An overview on intercell interference management in mobile cellular networks: From 2g to 5g," in *2014 IEEE International Conference on Communication Systems*, Nov. 2014, pp. 217–221. DOI: 10.1109/ICCS.2014.7024797.

[55] E. Hossain, M. Rasti, H. Tabassum, and A. Abdelnasser, "Evolution toward 5g multi-tier cellular wireless networks: An interference management perspective," *IEEE Wireless Communications*, vol. 21, no. 3, pp. 118–127, Jun. 2014, ISSN: 1558-0687. DOI: 10.1109/MWC.2014.6845056.

[56] M. S. Ali, "An overview on interference management in 3gpp LTE-advanced heterogeneous networks," *International Journal of Future Generation Communication and Networking*, vol. 8, pp. 55–68, Feb. 28, 2015. DOI: 10.14257/ijfgcn.2015.8.1.07.

[57] M. Cierny, H. Wang, R. Wichman, Z. Ding, and C. Wijting, "On number of almost blank subframes in heterogeneous cellular networks," *IEEE Transactions on Wireless Communications*, vol. 12, no. 10, pp. 5061–5073, Oct. 2013, ISSN: 1558-2248. DOI: 10.1109/TWC.2013.090513.121756.

[58] M. S. Ali, "On the evolution of coordinated multi-point (CoMP) transmission in LTE-advanced," *International Journal of Future Generation Communication and Networking*, vol. 7, no. 4, pp. 91–102, Aug. 31, 2014, ISSN: 22337857, 22337857. DOI: 10.14257/ijfgcn.2014.7.4.09.

[59] Y. Zhou, T. Ng, J. Wang, K. Higuchi, and M. Sawahashi, "Ofcdm: A promising broadband wireless access technique," *IEEE Communications Magazine*, vol. 46, no. 3, pp. 38–49, 2008.

[60] G. Zhai, L. Tian, Y. Zhou, and J. Shi, "Load diversity based optimal processing resource allocation for super base stations in centralized radio access networks," *Science China Information Sciences*, vol. 57, no. 4, pp. 1–12, Apr. 1, 2014, ISSN: 1869-1919. DOI: 10.1007/s11432-014-5075-y.

[61] Y. Zhou, T.-s. Ng, J. Wang, K. Higuchi, and M. Sawahashi, "OFCDM: A promising broadband wireless access technique," *IEEE Communications Magazine*, vol. 46, no. 3, pp. 38–49, Mar. 2008, ISSN: 1558-1896. DOI: 10.1109/MCOM.2008.4463770.

[62] V. R. Cadambe and S. A. Jafar, "Interference alignment and degrees of freedom of the k-user interference channel," *IEEE Transactions on Information Theory*, vol. 54, no. 8, pp. 3425–3441, Aug. 2008, ISSN: 1557-9654. DOI: 10.1109/TIT.2008.926344.

[63] C. M. Yetis, T. Gou, S. A. Jafar, and A. H. Kayran, "On feasibility of interference alignment in MIMO interference networks," *IEEE Transactions on Signal Processing*, vol. 58, no. 9, pp. 4771–4782, Sep. 2010, ISSN: 1941-0476. DOI: 10.1109/TSP.2010.2050480.

[64] O. El Ayach, S. W. Peters, and R. W. Heath, "The practical challenges of interference alignment," *IEEE Wireless Communications*, vol. 20, no. 1, pp. 35–42, Feb. 2013, ISSN: 1558-0687. DOI: 10.1109/MWC.2013.6472197.

[65] M. Razaviyayn, G. Lyubeznik, and Z.-Q. Luo, "On the degrees of freedom achievable through interference alignment in a MIMO interference channel," *IEEE Transactions on Signal Processing*, vol. 60, no. 2, pp. 812–821, Feb. 2012, ISSN: 1941-0476. DOI: 10.1109/TSP.2011.2173683.

[66] G. Bresler, D. Cartwright, and D. Tse, "Settling the feasibility of interference alignment for the MIMO interference channel: The symmetric square case," *arXiv:1104.0888 [cs, math]*, Apr. 5, 2011. arXiv: 1104.0888.

[67] S. A. Jafar, *Interference alignment: A new look at signal dimensions in a communication network*. Now Publishers Inc, 2011.

[68] N. Zhao, F. R. Yu, M. Jin, Q. Yan, and V. C. M. Leung, "Interference alignment and its applications: A survey, research issues, and challenges," *IEEE Communications Surveys Tutorials*, vol. 18, no. 3, pp. 1779–1803, 2016, ISSN: 1553-877X. DOI: 10.1109/COMST.2016.2547440.

[69] F. Pantisano, M. Bennis, W. Saad, M. Debbah, and M. Latva-aho, "Interference alignment for cooperative femtocell networks: A game-theoretic approach," *IEEE Transactions on Mobile Computing*, vol. 12, no. 11, pp. 2233–2246, Nov. 2013, ISSN: 1558-0660. DOI: 10.1109/TMC.2012.196.

[70] N. Zhao, F. R. Yu, H. Sun, A. Nallanathan, and H. Yin, "A novel interference alignment scheme based on sequential antenna switching in wireless networks," *IEEE Transactions on Wireless Communications*, vol. 12, no. 10, pp. 5008–5021, Oct. 2013, ISSN: 1558-2248. DOI: 10.1109/TWC.2013.090413.121731.

[71] A. Ghosh, N. Mangalvedhe, R. Ratasuk, B. Mondal, M. Cudak, *et al.*, "Heterogeneous cellular networks: From theory to practice," *IEEE Communications Magazine*, vol. 50, no. 6, pp. 54–64, Jun. 2012, ISSN: 1558-1896. DOI: 10.1109/MCOM.2012.6211486.

[72] V. Chandrasekhar, J. G. Andrews, and A. Gatherer, "Femtocell networks: A survey," *IEEE Communications Magazine*, vol. 46, no. 9, pp. 59–67, Sep. 2008, ISSN: 1558-1896. DOI: 10.1109/MCOM.2008.4623708.

[73] V. Chandrasekhar and J. G. Andrews, "Spectrum allocation in tiered cellular networks," *IEEE Transactions on Communications*, vol. 57, no. 10, pp. 3059–3068, Oct. 2009, ISSN: 1558-0857. DOI: 10.1109/TCOMM.2009.10.080529.

[74] M. Y. Arslan, J. Yoon, K. Sundaresan, S. V. Krishnamurthy, and S. Banerjee, "A resource management system for interference mitigation in enterprise OFDMA femtocells," *IEEE/ACM Transactions on Networking*, vol. 21, no. 5, pp. 1447–1460, Oct. 2013, ISSN: 1558-2566. DOI: 10.1109/TNET.2012.2226245.

[75] W. Shin, N. Lee, J.-B. Lim, C. Shin, and K. Jang, "On the design of interference alignment scheme for two-cell MIMO interfering broadcast channels," *IEEE Transactions on Wireless Communications*, vol. 10, no. 2, pp. 437–442, Feb. 2011, ISSN: 1558-2248. DOI: 10.1109/TWC.2011.120810.101097.

[76] C. Suh, M. Ho, and D. N. C. Tse, "Downlink interference alignment," *IEEE Transactions on Communications*, vol. 59, no. 9, pp. 2616–2626, Sep. 2011, ISSN: 1558-0857. DOI: 10.1109/TCOMM.2011.070511.100313.

[77] L. Ruan, V. K. N. Lau, and M. Z. Win, "The feasibility conditions for interference alignment in MIMO networks," *IEEE Transactions on Signal Processing*, vol. 61, no. 8, pp. 2066–2077, Apr. 2013, Conference Name: IEEE Transactions on Signal Processing, ISSN: 1941-0476. DOI: 10.1109/TSP.2013.2241056.

[78] S. Ben Halima and A. Saadani, "Joint clustering and interference alignment for overloaded femtocell networks," in *2012 IEEE Wireless Communications and Networking Conference (WCNC)*, ISSN: 1558-2612, Apr. 2012, pp. 1229–1233. DOI: 10.1109/WCNC.2012.6213965.

[79] M. Maso, M. Debbah, and L. Vangelista, "A distributed approach to interference alignment in OFDM-based two-tiered networks," *IEEE Transactions on Vehicular Technology*, vol. 62, no. 5, pp. 1935–1949, Jun. 2013, Conference Name: IEEE Transactions on Vehicular Technology. DOI: 10.1109/TVT.2013.2245516.

[80] W. Shin, W. Noh, K. Jang, and H.-H. Choi, "Hierarchical interference alignment for downlink heterogeneous networks," *IEEE Transactions on Wireless Communications*, vol. 11, no. 12, pp. 4549–4559, Dec. 2012, Conference Name: IEEE Transactions on Wireless Communications, ISSN: 1558-2248. DOI: 10.1109/TWC.2012.101912.120421.